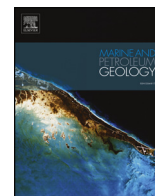




ELSEVIER

Contents lists available at ScienceDirect

## Marine and Petroleum Geology

journal homepage: [www.elsevier.com/locate/marpetgeo](http://www.elsevier.com/locate/marpetgeo)

Research paper

## New constraints on the age of the opening of the South Atlantic basin

Stuart A. Hall<sup>a,\*</sup>, Dale E. Bird<sup>a,b</sup>, David J. McLean<sup>c</sup>, Philip J. Towle<sup>c</sup>, James V. Grant<sup>d</sup>, Hunter A. Danque<sup>c</sup><sup>a</sup> Department of Earth & Atmospheric Sciences, University of Houston, Houston, TX, 77204, USA<sup>b</sup> Bird Geophysical DBA, 16903 Clan Macintosh, Houston, TX 77084, USA<sup>c</sup> Anadarko Petroleum Corporation, 1201 Lake Robbins Drive, The Woodlands, Texas, 77380, USA<sup>d</sup> Chesapeake Energy Corporation, P.O. Box 18496, Oklahoma City, OK, 73154-0496, USA

## ARTICLE INFO

## Keywords:

Seafloor spreading  
Plate tectonics  
Continental breakup

## ABSTRACT

Detailed, high quality, marine total field magnetic data recently acquired over parts of the South Atlantic Ocean off the southwestern margin of South Africa display a pattern of well-defined, NW-SE striking linear magnetic anomalies that can be traced with confidence over distances > 150 km. The magnetic anomalies are interpreted to be M-series seafloor spreading anomalies M9 to M11, which are consistent with the initiation of seafloor spreading at approximately 135 Ma (Late Valanginian/Early Hauterivian). Seafloor spreading models indicate a more rapid (44 mm/yr) initial spreading phase between M11 and M4/M5 followed by slower (29 mm/yr) spreading from M4/M5 to M0. This two rate spreading model also matches M-series anomalies previously reported over the conjugate South American margin offshore Argentina where the rates are slightly (< 10%) slower. The presence of M11 anomalies over both margins suggests an earlier opening of the southern South Atlantic basin than previously recognized.

Breaks in the continuity of the linear anomaly pattern, observed in map view, are oriented approximately NE-SW and are considered sites of possible fracture zones. One such discontinuity, which we have termed the “Cape Lineament” (CL), marks a significant change in crustal character and Cretaceous depositional history, as revealed by gravity data and seismic reflection data, respectively. Crust NW of the CL, in the Orange Basin, is characterized by greater thickness and the presence of seismically-imaged seaward dipping reflectors (SDRs) whereas SE of the CL the crust has a more “normal” oceanic thickness and SDRs are either absent or more limited in areal extent. Magnetic, gravity and seismic data were combined to develop a crustal model of the South African margin north of the CL that includes: (a) a region of rifted/attenuated continental crust landward of magnetic anomaly G, (b) a 60–80 km wide zone of substantially intruded, underplated thin continental crust overlain by SDRs between anomalies G and M11, and (c) a ~90 km wide zone of thick oceanic crust associated with a wide intrusion zone and smoother seafloor spreading magnetic anomalies that thins progressively to normal oceanic crustal thickness at the seaward edge of the overlying SDRs. South of the CL, the change in crustal character from attenuated continental crust to normal thickness oceanic crust occurs over a much shorter distance of approximately 35–40 km, possibly indicating the diminished influence of magmatic material. Although linear magnetic anomalies are observed both NW and SE of CL, anomalies to the SE display a better correlation with those predicted by our seafloor spreading model.

We have successfully reconstructed the positions of the African and South American margins south of 32°S at M11 time (i.e., ~135 Ma) using a new rotation pole at 38.86°N, 31.46°W. This pole applies only to the southernmost margins of the Austral segment where M11 is observed. Further north at this time the margins are undergoing non-rigid deformation that includes both crustal extension and magmatic underplating.

## 1. Introduction

The breakup of Gondwana that began with the rifting of Antarctica away from Africa in the Early Jurassic (Eagles and König, 2008; König and Jokat, 2010; Leinweber and Jokat, 2012; Gaina et al., 2013;

Nguyen et al., 2016) was followed by the Late Jurassic-Early Cretaceous rifting of South America and southern Africa (Heine et al., 2013) that led to the formation of the South Atlantic basin (Rabinowitz and LaBrecque, 1979; Unternehr et al., 1988; Nürnberg and Müller, 1991; Gladchenko et al., 1997; Jokat et al., 2003; McDonald et al., 2003;

\* Corresponding author.

E-mail address: [sahgeo@uh.edu](mailto:sahgeo@uh.edu) (S.A. Hall).<https://doi.org/10.1016/j.marpetgeo.2018.03.010>

Received 4 December 2017; Received in revised form 22 February 2018; Accepted 7 March 2018

Available online 09 March 2018

0264-8172/© 2018 Elsevier Ltd. All rights reserved.

Perez-Diaz and Eagles, 2014; Koopmann et al., 2014a; Granot and Dymant, 2015). When seafloor spreading began, the amount of extension prior to spreading, and the nature of the margins (volcanic or non-volcanic) are important constraints on developing a detailed tectonic history of the region.

Magnetic anomalies over the margins of the Austral segment of the South Atlantic basin suggest that seafloor spreading began earlier in the southernmost portion of the basin and progressed northward (Rabinowitz and LaBrecque, 1979; Martin, 1984; Corner et al., 2002; Franke et al., 2010; Moulin et al., 2010; Franke, 2013). Anomalies M0 to M4 have been mapped over both margins of the segment from the Rio Grande Fracture Zone (RGFZ) south to the Falkland Plateau/Ewing Bank in the west and from the Walvis Ridge to Cape Agulhas in the east (Larson and Ladd, 1973; Rabinowitz, 1976; Cande and Rabinowitz, 1978; Rabinowitz and LaBrecque, 1979; LaBrecque and Hayes, 1979; Martin et al., 1982; Nürnberg and Müller, 1991; Max et al., 1999; Koopmann et al., 2014b; Corner et al., 2002; Moulin et al., 2010; Bird and Hall, 2010; Hall et al., 2014). Using limited data coverage, Cande and Rabinowitz (1978) were able to tentatively identify anomalies M3 and M4 north of the RGFZ. More recently, Bird and Hall (2016) using more extensive, recently acquired magnetic data have identified M3 and M4 as far north as 21°S on the South American side.

The distribution of pre-M4 anomalies over either margin is not as well documented. Over the southernmost portion of the African margin, Rabinowitz and LaBrecque (1979) were able to identify magnetochrons M7 to M11 confidently to 33° S and possibly as far north as 30°S. Subsequent analyses of more recently acquired, detailed magnetic data along the southwest African margin suggest that M11 may be traced further north to possibly 24°S (Corner et al., 2002) but its identification is uncertain (Moulin et al., 2010). Further south, high quality magnetic data recently acquired by the German Federal Institute for Geosciences and Natural Resources (BGR) have allowed M0 to M9 to be mapped with confidence from 35°S north to 32.5°S (Koopmann et al., 2014b). Over the South American margin, Rabinowitz and LaBrecque (1979) found difficulty in correlating anomalies west of their M4 isochron with those predicted by their seafloor spreading model. Later, with more detailed aeromagnetic data, Max et al. (1999) were able to map linear anomalies over the South American margin between 38°S and 45°S roughly parallel to the coast. Over the Argentinian margin, between 43.5° and 44.5°S, these anomalies were subsequently identified by Schreckenberger et al. (2002) as magnetochrons M2 to M10. Thus, while anomalies M9 and older have been identified over portions of the southernmost Austral segment they have not been identified with confidence north of ~32°S on the African margin nor north of ~43°S over the South American margin. These observations are consistent with either i) a northward decrease in the age of the oldest oceanic crust or ii) a substantial and rapid northward decrease in spreading rate. Such a spreading rate change, however, is not consistent with published poles of rotation for the early opening of the South Atlantic (e.g., Eagles, 2007; Hall and Bird, 2007; Torsvik et al., 2009; Moulin et al., 2010; Perez-Diaz and Eagles, 2014; Hall et al., 2014; Bird and Hall, 2016). In addition, a pole position that resulted in a rapid change in spreading rate would be much closer to the South Atlantic and produce strongly curved fracture zones that are not apparent in the satellite gravity data (Sandwell et al., 2014), although more curved fracture zones have been suggested by Bolli et al. (1978).

Although the potential age difference is modest (~5My) i.e., from M11 - Late Valanginian/Early Hauterivian (~136 Ma) to M4 - Late Hauterivian/early Barremian (~131 Ma), the amount of motion is significant. Using published half spreading rates of 30–40 mm/yr (Schreckenberger et al., 2002; Bird and Hall, 2010, 2016; Hall et al., 2014) suggests a total Africa-South America separation greater than 300 km must be accommodated. To explain the discrepancy in the amount and age of oceanic crust, and to accommodate a diachronous opening of the South Atlantic, several authors have proposed models that involve deformation along various intraplate tectonic zones and/or

motion along continental strike slip or transfer faults (e.g., Curie, 1984; Unternehr et al., 1988; Nürnberg and Müller, 1991; Eyles and Eyles, 1993; König and Jokat, 2006; Eagles, 2007; Moulin et al., 2010; Torsvik et al., 2009; Perez-Diaz and Eagles, 2014). Although these intra-plate boundaries are inferred to be active prior to M4 time, their location and the amount, timing and duration of motion are not well constrained. Rigid plate reconstructions that do not include this deformation and/or motions lead to gaps and overlaps in the pre-drift fit of southern Africa and South America (Nürnberg and Müller, 1991; Lawver et al., 1998; König and Jokat, 2006; Moulin et al., 2010; Heine et al., 2013; Quirk et al., 2013). However, many of these reconstructions are based upon the location of a continent-ocean boundary (COB) that is poorly defined. As a consequence, it is difficult to assess how much of these “misfits” are due to motion on these intra-plate features and how much are the result of the poor definition of the COB along the margins and the amount of crustal extension prior to the onset of seafloor spreading. Defining the COB and identifying M-series anomalies is hampered in part by the presence of extensive areas of volcanic flows, expressed as seaward dipping reflectors (SDRs) on regional seismic reflection data, that extend over the margins by more than 200 km in an east-west direction in map view on the African side (Bauer et al., 2000; Corner et al., 2002; Hirsch et al., 2009; Koopmann et al., 2014b; Towle et al., 2015) and more than 150 km on the South American side (Franke et al., 2007, 2010; Becker et al., 2014).

In order to evaluate models for the evolution of the South Atlantic basin, better constraints regarding the age and amount of pre-M4 oceanic crust and the amount of crustal extension along both margins are required. Here we present the results from a new marine magnetic survey over the continental margin of SW Africa and discuss their implications for the early breakup history of the southernmost portion of the ocean basin between Africa and South America.

## 2. Data

The data used in this study consist of a new marine seismic reflection, magnetic and gravity survey (2012–13) over the continental margin of SW Africa (Figs. 1 and 2), PGS multi-client seismic reflection, magnetic and gravity data acquired in 2002, regional GEODAS magnetic lines, limited well and seismic refraction data, and recently published satellite gravity data (Sandwell et al., 2014).

### 2.1. Magnetic data

The new proprietary magnetic survey was acquired as part of a marine 2-D seismic, gravity and magnetic survey by Anadarko Petroleum Corporation as part of a petroleum exploration joint venture with PetroSA. The survey was conducted between November 2012 and February 2013 and consisted of 54 lines totaling more than 6400 km. Ten of these lines were oriented along N 50 °E in the northern portion of the survey area, and 38 lines oriented along N 30 °E in central and southern portions (Fig. 3a). The line spacing was approximately 6 km. Four tie lines (not shown in Fig. 3a) with line separations between 10 and 15 km and a roughly NW-SE orientation were also acquired together with 2 well/borehole tie lines with orientations of N35E and N80E. A SeaSPY magnetometer system with an Overhauser magnetometer sensor was used to acquire magnetic data. The primary and secondary navigation systems on the survey were CNAV RTG and VERIPOS Ultra respectively and thus positional accuracy was excellent.

The PGS data were acquired in 2002 as part of a multi-client 2-D seismic, gravity and magnetic survey. The survey comprises 21 individual lines totaling 2250 km acquired with similar orientations to those of the 2012/13 survey (Fig. 3a). The data were acquired using an Elsec Proton Magnetometer Model 7706. The primary navigation and surface positioning of the vessel was achieved utilizing a Seadiff DGPS system and thus positioning accuracy was also excellent for this survey.

The GEODAS magnetic data have various orientations and were

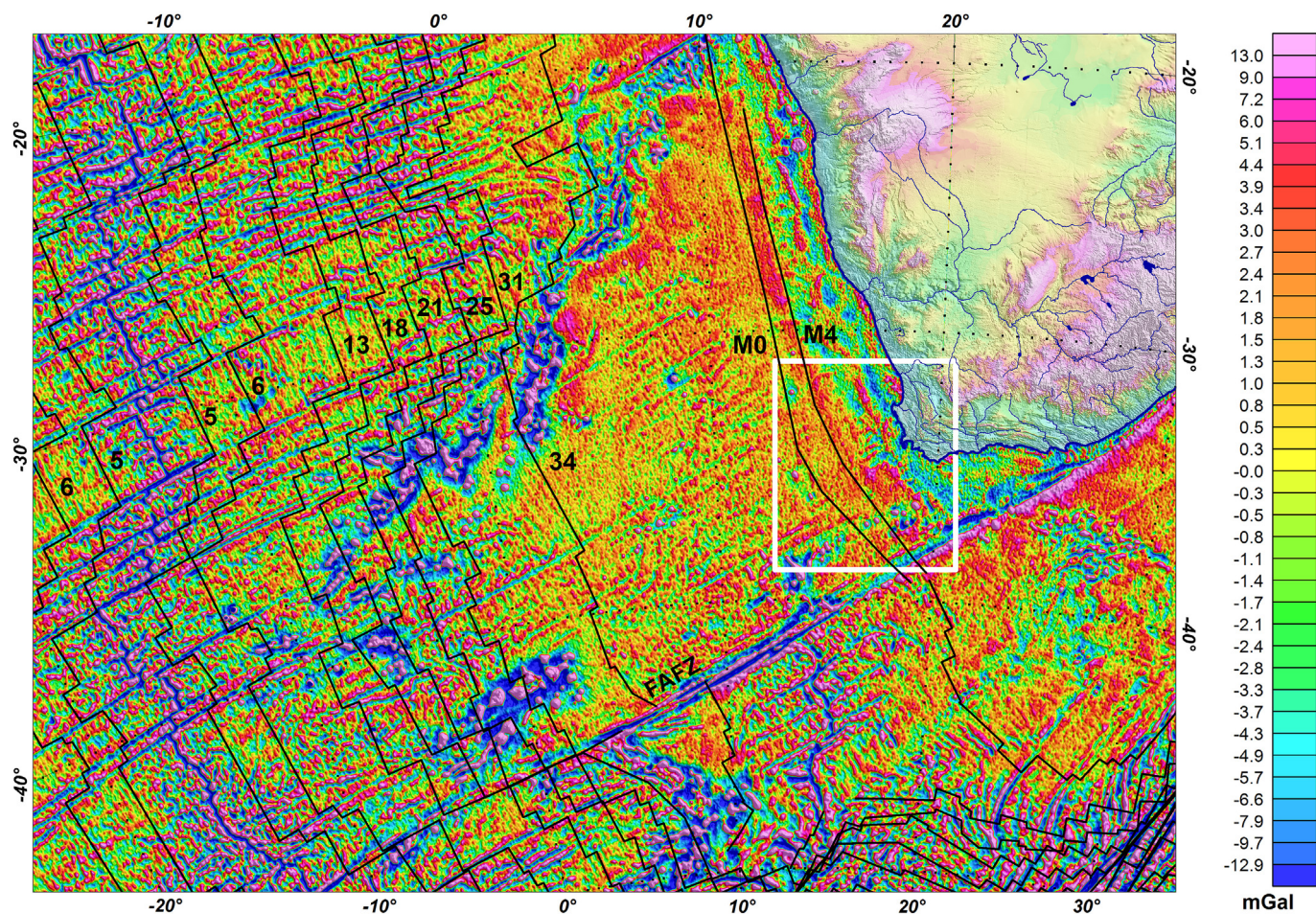


**Fig. 1.** Residual satellite-derived Bouguer gravity anomalies over the South Atlantic Ocean and African topography. Residual anomalies (also in Fig. 2) are calculated by subtracting upward continued (6 km) Bouguer anomalies from original Bouguer anomalies. GTOPO30 topography (also in Figs. 2 and 3) color bar is displayed in Fig. 3a. Geomagnetic isochrons (Müller et al., 1997), including labels, are heavy black lines. FAFZ show the location of the Falklands-Agulhas Fracture Zone. Location of Fig. 2 is shown by the white box. The coordinate system for all maps, except Fig. 9, is UTM 33 South, WGS84.

gathered over a period of more than 50 years using a variety of instrumentation and often using earlier, less accurate navigational systems.

## 2.2. Marine gravity and seismic reflection data

Proprietary 2-D seismic reflection and marine gravity data were acquired at the same time as the proprietary magnetic data. The seismic data were recorded using a 10,000 m cable consisting of 800 channels with 12.5 m separation and towed at a depth of 18 m. The source was a 4330 in<sup>3</sup>, 2000 p.s.i., tuned Sercel Sodera airgun array towed at a depth of 12 m. The data were processed in time and converted to depth using a velocity function derived from seismic stacking velocities and constrained by available well data. The data were recorded continuously with shots every 9.5 or 10.0 s and a nominal record length of 16.058 s. Shot and swell noise, however, limited depth imaging to 20 km.

The gravity data were recorded using a LaCoste and Romberg Model S Marine Gravity Meter, S/N S-78 with UltraSys upgrade.

## 2.3. Satellite gravity data

Global gravity anomalies, free to download from Scripps Institution of Oceanography, consist of satellite-derived free air gravity anomalies over marine areas (Sandwell et al., 2014), and Earth Gravitational Model 2008 over land areas (Pavlis et al., 2012). New CryoSat-2 and Jason-1 satellite geodetic mission data (Sandwell et al., 2014),

combined with existing Geosat and ERS-1 geodetic mission data (Sandwell and Smith, 1997), have improved the resolution of the satellite data by a factor of 2–4, with amplitude resolution increasing from 3 to 5 mGal to about ~2 mGal, largely due to advances in radar technology where range precision is increased by 1.25 times (Sandwell et al., 2014) as well as the greater number of passes by adding the new CryoSat-2 and Jason-1 data to the original Geosat and ERS-1 data.

## 2.4. Well and seismic refraction data

There are thirty-eight industry wells along the western Atlantic margin of the Republic of South Africa at the time of this writing. Two DSDP boreholes (Leg 40, Sites 360 and 361) were drilled in 1975 (Bollini et al., 1978) in the study area (Fig. 2). Two of the thirty-eight wells are highlighted in this study: Soekor O-A1/Z1 and Soekor C-B1. Well O-A1/Z1, in water depth of 744 m, penetrated basalts interbedded with sediments at 4177 m subsea true vertical depth. Well C-B1, in water depth 387 m, penetrated metamorphic-grade rocks at 1851 m subsea true vertical depth. These crystalline rocks are interpreted to be of oceanic crustal affinity and continental crustal affinity, respectively. DSDP 361 stopped drilling approximately 100 m above projected crystalline basement in Aptian sediments (Bollini et al., 1978). The basement section appears to be uniform, smooth oceanic crust at the DSDP 361 location based on its 2D seismic character within the new 2D seismic survey. These borehole penetrations of basement (and near basement) rocks are used to assist in calibration of the 2D gravity models presented in the

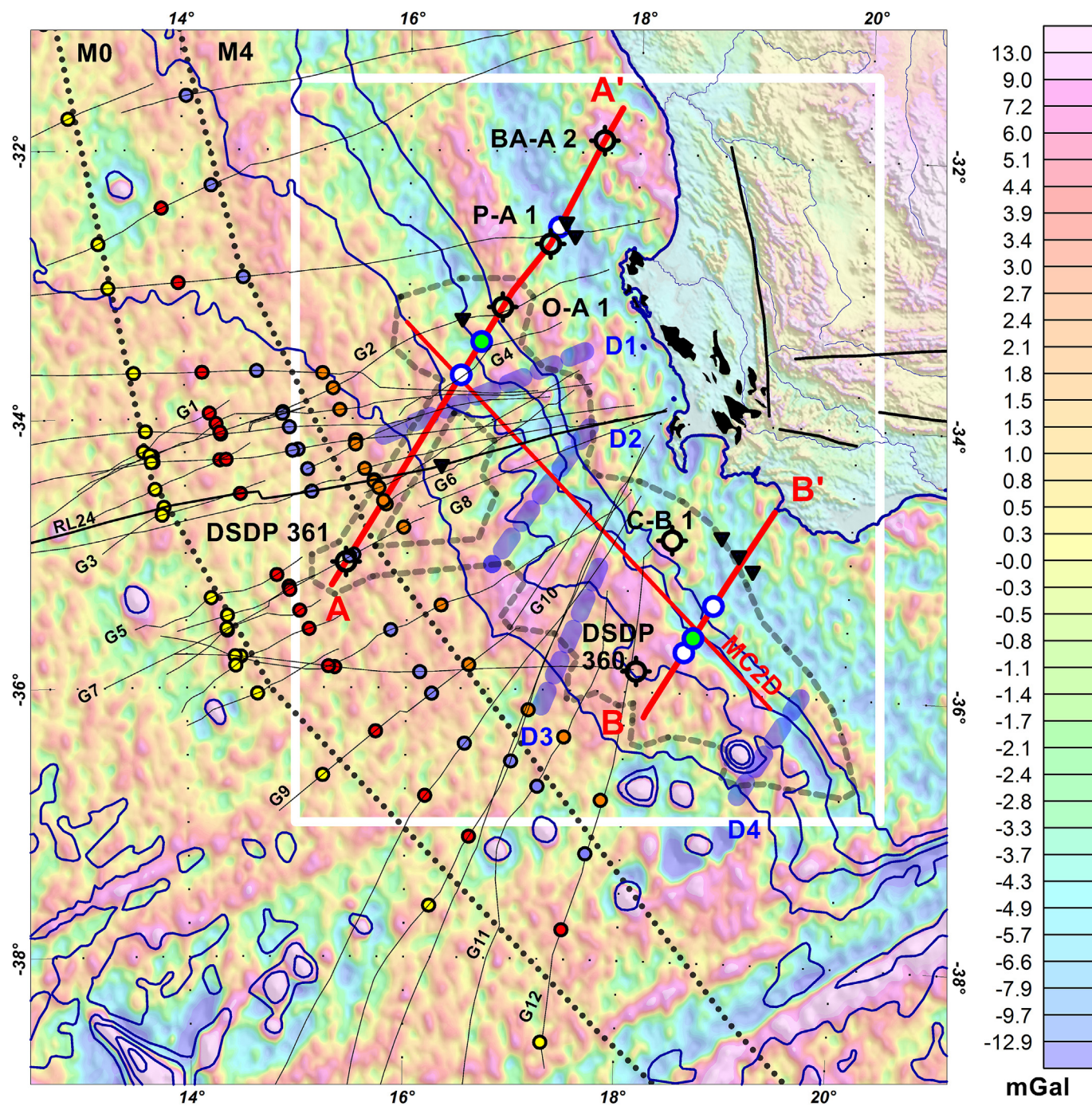


Fig. 2. Residual satellite-derived Bouguer gravity anomalies over the South Atlantic Ocean and African topography. Residual anomaly calculation described in Fig. 1. GTOPO30 topography (also in Figs. 1 and 3) color bar is displayed in Fig. 3a. The seismic reflection line (MC2D) displayed in Fig. 4 is red; Seismic refraction data are inverted triangles; wells are borehole symbols (including well names); magnetic chron picks are color-filled circles (see Table 1) located on open-file marine tracklines (thin black); and the location of Fig. 3 is shown by the white box.

Interpretation section.

Published results from refraction experiments (Hayes et al., 1991) were used to control basement depths in 2D gravity models. Modeled basement depths are constrained by three stations projected into Model A-A' and two stations projected into Model B-B' (shown in Fig. 3a).

3. Results

3.1. Profile to profile correlations of magnetic data

Magnetic anomalies observed over much of the new survey area

have amplitudes of 150–200 nT and peak to trough distances of 10–20 km. Towards the coast, the anomaly amplitudes are significantly smaller and many profiles are relatively flat. Individual magnetic anomaly features can be correlated from line to line throughout much of the new survey area (Fig. 3a). These correlations, augmented with GEODAS lines that cross the area, display a pattern of linear anomalies striking approximately N 40° W (Fig. 3a). Examples of dominant features that can be traced over several profiles, which have been color-coded to document their continuity, are shown in Fig. 3b. Over the southern part of the survey area individual features can be traced with confidence over distances of several 10's km up to more than 170 km

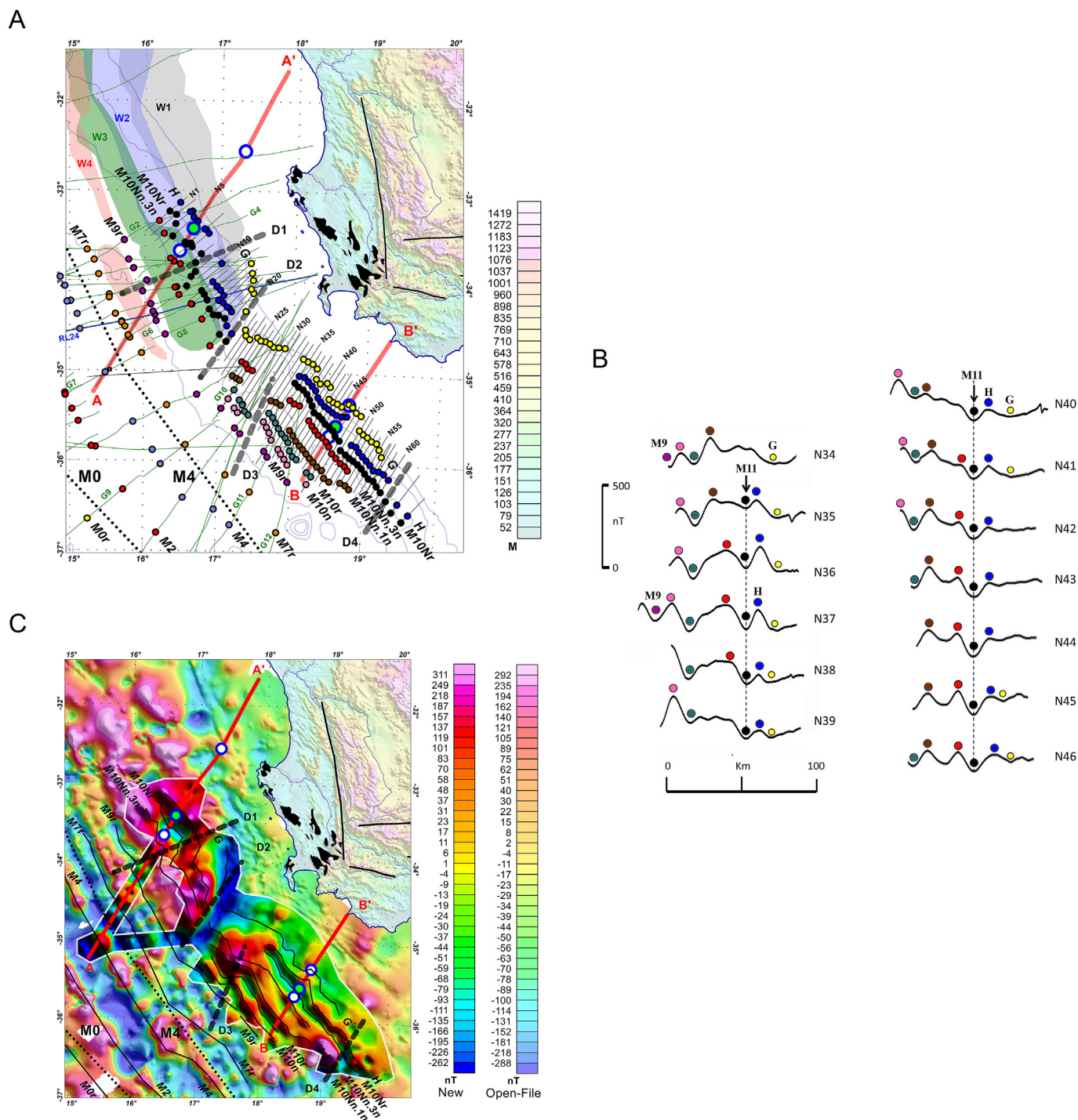


**Fig. 3.** a – Magnetic chron identification and African topography (GTOPO30). Labeled magnetic chron picks are color-filled circles (see Table 1) located on open-file (thin green) and new marine tracklines (thin black); for Rabinowitz and LaBrecque (1979) profile 24; SDR wedges 1 through 4 (W1 – W4, modified after Koopman et al., 2014) are represented by gray, blue, green and red shaded polygons respectively. Common elements in Figs. 2 and 3 are described in Fig. 2 caption. b – A sample of the correlations of total intensity magnetic anomaly profiles over a portion of the study area. Locations of profiles are shown in (a). Color filled circles trace the correlations of individual features. Magnetic minimum (solid black circle) is interpreted as the M11 magnetochron from Rabinowitz and LaBrecque (1979). c – Total magnetic intensity anomalies and African topography. Reprocessed open-file marine magnetic anomalies (Bird Geophysical) are overlain by new, high-resolution magnetic anomalies (Anadarko Petroleum Corporation); GTOPO30 topography (also in Figs. 1 and 2) color bar is displayed in Fig. 3a. New high-resolution marine magnetic data survey outline is white; labeled magnetic isochron line correlations from this study are black lines (see Fig. 3a). Common elements in Figs. 2 and 3 are described in Fig. 2 caption.

(Fig. 3a). A prominent minimum, (shown as solid black circles in Fig. 3a and b), can be traced from line N35 to the southern limit of the survey. Similar anomalies are observed over the northern half of the survey area but there are fewer correlatable features and individual features

can be correlated from line to line over shorter distances (Fig. 3a). High amplitude anomalies are observed over portions of Lines N28 to N33 and over the seaward ends of Lines N57 to N60, which display a ~1200 nT peak (Fig. 3a and c).

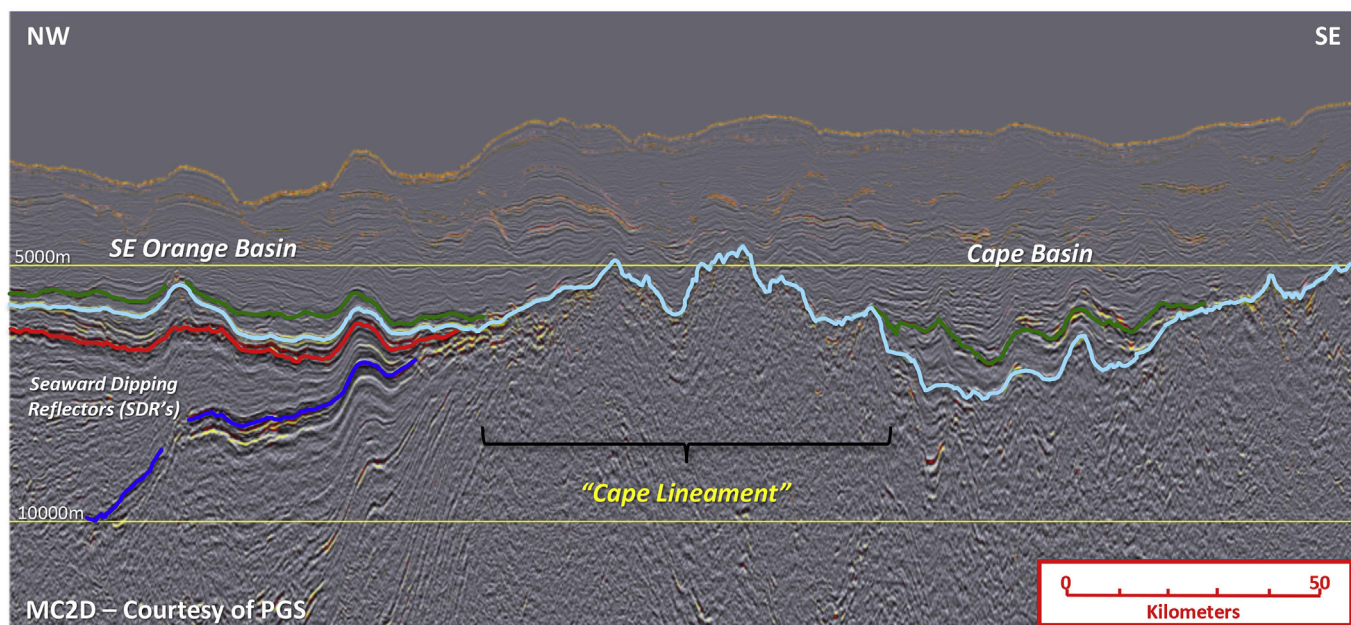


Fig. 4. 2D seismic reflection data (in depth) oriented northwest to southeast across the Cape Lineament. The Cape Lineament is manifested as a pronounced structural arch or ridge that separates the Orange Basin to the northwest from the Cape Basin to the south east. Note the well-developed sequence of SDRs to the northwest of the Cape Lineament and the variation in sedimentary thickness between the Orange and Cape Basins. The base of post rift sediments is shown by thick light blue marker. Red, dark blue and yellow markers are regional intra-SDR events. Dark green marker is early Cretaceous event. The location of the profile is shown in Fig. 2.

### 3.2. Discontinuities

The continuity of the line-to-line correlations is interrupted in several places where the linear pattern is offset, generally in a NE-SW direction (Fig. 3a). Four separate discontinuities (labeled D1 to D4 in Fig. 3a) have been identified across the study area. Discontinuities D3 and D4 are adjacent to areas with broad, large amplitude magnetic anomalies (Fig. 3c).

**Discontinuity D1:** Anomaly amplitudes decrease significantly on Lines N9, N10 and N11 and the linear features identified undergo a right-lateral offset between Lines N8 and N12. Although all linear features are offset in the same sense, individual features are offset by differing amounts with those closer to the coast offset by ~30–35 km whereas those further offshore are only offset by 15–20 km. Anomaly M9 previously mapped from regional magnetic data shows only a minor offset ( $\leq 10$  km) but with the same sense. Anomalies M7, M4, and M0 appear to be continuous across the area. The trend of the discontinuity is  $\sim N60^\circ - N65^\circ$  (Fig. 3a).

**Discontinuity D2:** There is a broad region between lines N19 and N24 of the new survey where linear anomalies cannot be identified with confidence. This region includes a prominent magnetic low that cuts across the entire survey area in a  $N 35^\circ E$  direction and continues seaward of the survey limits (Fig. 3c). Although the linear anomalies are discontinuous across this feature, M-series anomalies M0, M2 and M4 identified further offshore from regional ship track data are continuous and do not display any significant offset. This discontinuity coincides with a major structure identified in the seismic reflection data, herein referred to as the Cape Lineament, which is described below.

**Discontinuity D3:** At this discontinuity, several prominent features are offset in a left-lateral sense by ~25 km between lines N31 and N34 (Fig. 3a). The discontinuity has a trend of  $N 35-40^\circ E$  and can be followed landward until it truncates against a strong positive anomaly (Fig. 3c), which is interpreted to be produced by a conical volcano observed on seismic reflection data. Linear magnetic anomalies M7 and M4, mapped further seaward from regional magnetic data (e.g., Koopmann et al., 2014a), also display a roughly 30 km left lateral offset in this area. Discontinuity D3 coincides with a feature identified as a

fracture zone by Larson and Ladd (1973) and Rabinowitz (1976) that also offsets M0 and is sometimes referred to as the Hope Fracture Zone.

**Discontinuity D4:** Discontinuity D4 is not well defined by the new data. Correlations of magnetic anomalies towards the southern limit of the new data are difficult because the survey lines are short and regional GEODAS lines with complete magnetic data are very oblique to the trend of the magnetic lineations. The well-defined magnetic minimum that can be traced ~170 km from Line N35 is abruptly truncated at Line N60 where it encounters a large positive anomaly and appears to be offset in a right lateral sense by ~20 km (Fig. 3a and c). Discontinuity D4 also coincides roughly with a portion of the Struisbaai FZ (Bolti et al., 1978).

### 3.3. Gravity data

Satellite-derived free air gravity anomalies (Sandwell et al., 2014) and Bouguer gravity anomalies are included with our supplementary material. To calculate Bouguer anomalies, we assumed the water bottom sediment density to be 2.0 g/cc, and have added 0.97 g/cc to the water layer. The residual Bouguer anomalies generated by subtracting 6 km upward continued Bouguer data from the original Bouguer data (Figs. 1 and 2) display several remarkable new details.

The active Mid-Atlantic Ridge (MAR) seafloor spreading center and extinct Cape Rise spreading center, located just south of the Falkland Agulhas Fracture Zone (FAFZ) and our study area can be clearly observed (Fig. 1). Likewise, the NNE oriented Walvis Ridge hotspot chain of seamounts is easily recognizable. The level of detail might best be understood by examining the ocean floor east of MAR and west of the Walvis Ridge, around annotated isochrons 5 to 18. A linear fabric, oriented subparallel to MAR, gives one an actual sense of seafloor accretion. Oceanic fracture zones, that orthogonally offset MAR segments, are also easily recognized and can be traced landward to M0.

Fracture zones expressions become subtle in our study area, but NE-SW trending linear features, that are in-line with fracture zone trends, can be mapped just north of a line of small seamounts between D3 and D4 (Fig. 2). Further north, short linear segments in-line with fracture zone trends are observed between D1 and D2. The Cape Lineament

(D2), as mapped from seismic data (Fig. 4), is structurally high. A relatively broad gravity low partially coincides with the lineament and suggests that the structure is rooted in the upper mantle, and may be isostatically compensated. Of the four discontinuities defined by magnetic anomaly offsets, only D1 is parallel to fracture zone trends farther offshore in the oceanic crust.

### 3.4. Seismic data

The high quality, long offset, deep penetration 2D seismic data, integrated with the high-resolution marine gravity and magnetic data, have allowed a re-evaluation of the crustal structure of the southwestern margin of South Africa. These data enable the differentiation of this part of the South Atlantic into two sectors. A northern sector that is contiguous with the greater Orange Basin, where SDRs are ubiquitous, and a southern sector, the Cape Basin, where SDRs are absent or poorly developed. These sectors are separated by a regional NE-SW trending structural ridge or discontinuity, which we have termed the “Cape Lineament” (Fig. 4). The northeasterly trend of the Cape Lineament can be projected landward and appears to coincide with the “Cape Syntaxis” (Fig. 3a) (Johnston, 2000; Paton et al., 2017a) portion of the Cape Fold Belt (CFB), which is exposed onshore in southern South Africa.

## 4. Interpretation

### 4.1. Seafloor spreading models and isochron identification

Since the early work by Rabinowitz and LaBrecque (1979) on the seafloor spreading history of the South Atlantic, several geomagnetic reversal time scales have been proposed for the Late Jurassic–Early Cretaceous portion of the time scale (e.g., Channell et al., 1995; Gradstein et al., 2004; Tominaga and Sager, 2010; Malinverno et al., 2012; Gradstein et al., 2012). All of these more recent time scales differ significantly from the Larson and Hilde (1975) scale used by Rabinowitz and LaBrecque (1979). However, these more recent time scales are somewhat similar to each other. We have used the time scale of Gradstein et al. (2012) to determine the seafloor spreading history on the basis that it is the most recent time scale widely adopted by the scientific community. A more recent geologic time scale (Ogg et al., 2016) has been published during the preparation of this work. The geomagnetic reversal time scale of this new time scale is identical to that of Gradstein et al. (2012). For the M-series anomalies involved in this study, there are 2 major differences between the Gradstein et al. (2012) scale and earlier one of Larson and Hilde (1975): (1) the age of the M0 anomaly is significantly older (viz 126 Ma vs 109 Ma), and (2) the roughly 9 My time interval between M0 and M11 on this scale is substantially shorter than the corresponding 17 My of the earlier scale. As a result of the shorter M0–M11 time interval, seafloor spreading models developed here involve faster spreading rates, which are consistent with more recent analyses (e.g., Schreckenberger et al., 2002). It is worth noting that the magnetic minimum identified by Rabinowitz and LaBrecque (1979) as M11 corresponds to M10Nr on the Gradstein et al. (2012) scale with a proposed age of 135 Ma. For simplicity, we have adopted the prior M11 terminology here.

A broad regional framework for the interpretation of the magnetic anomalies was established using several long GEODAS lines that either join or overlap the new survey data (Fig. 5). These GEODAS lines encompass the younger M-series anomalies (from M0 up to M9) and enable older M anomalies (M7, M9 and M11) observed on the new data to be identified with some confidence. We have used Line N5, which extends further seaward than other new survey lines, to correlate with features identified as M4, M7, M9 and M11 by Rabinowitz and LaBrecque (1979) on their Profile 24 (Fig. 5). The excellent correlation of our new data with Profile 24 allows these M features to be mapped on lines throughout much of the new survey area.

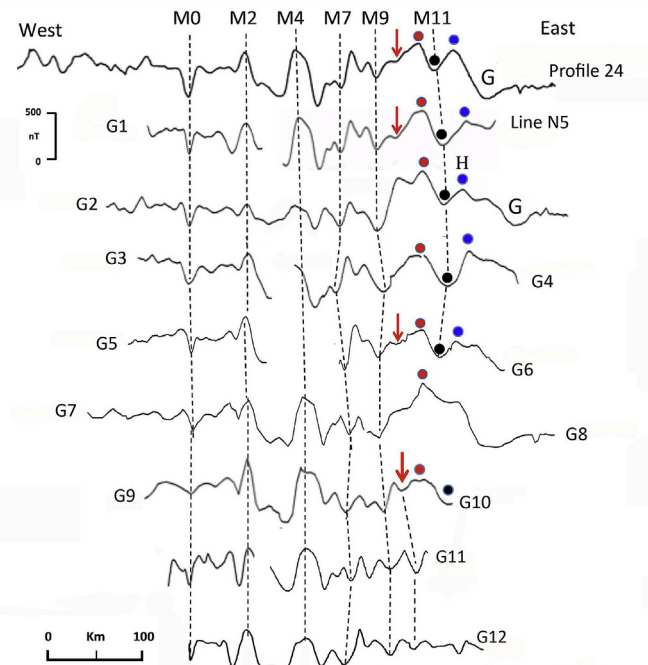


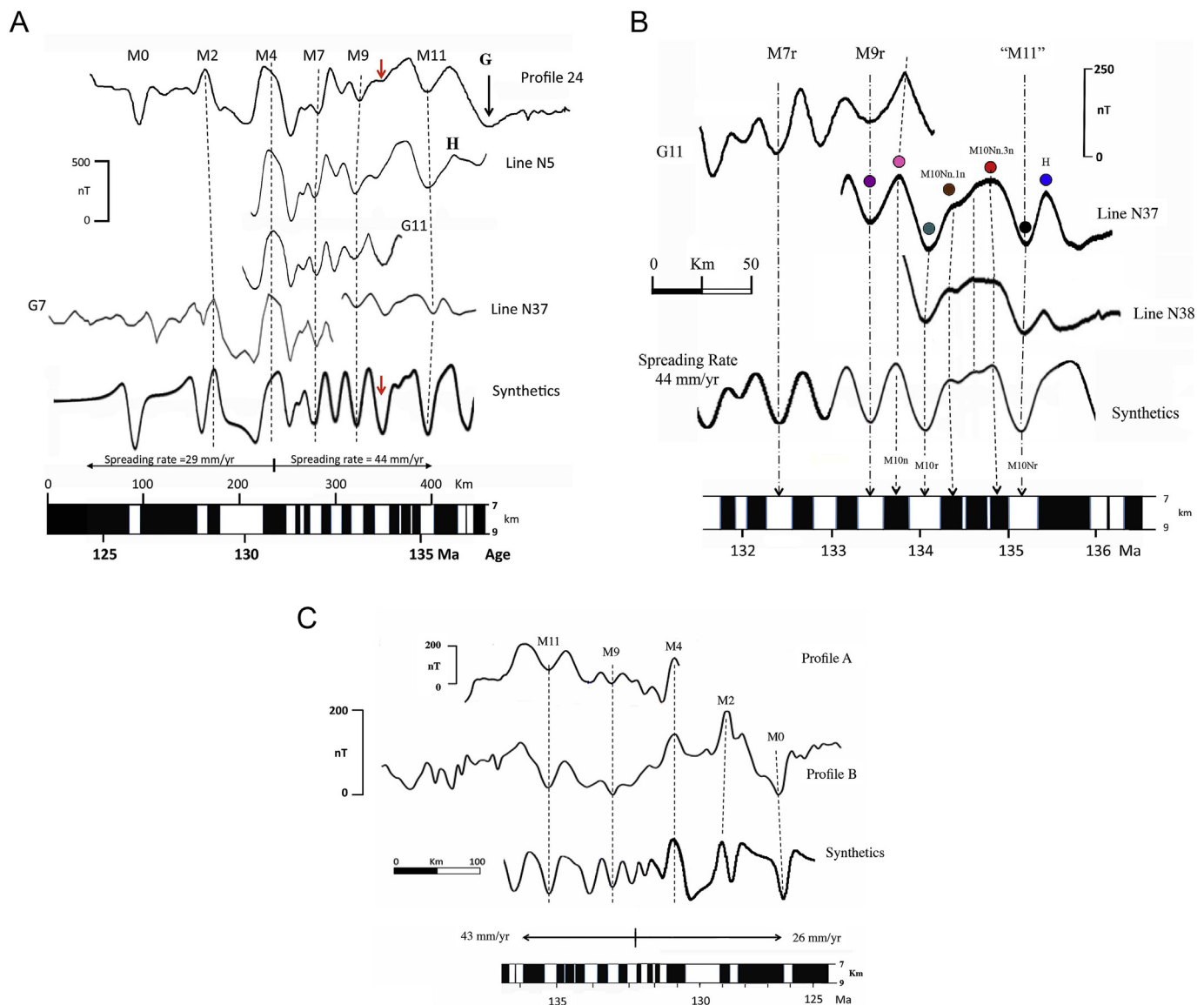
Fig. 5. Regional framework of correlated magnetic anomaly profiles showing identification of M-series anomalies. Locations of the GEODAS lines are shown in Fig. 2. Profile 24 is from Rabinowitz and LaBrecque (1979). Color filled circles display interpreted seafloor spreading anomalies M10Nn.3n (red), and “M11” (black). Anomaly H is shown as a dark blue filled circle. Red arrow indicates a local minimum that is interpreted as M10r.

Fig. 5 shows a double-peaked feature between M7 and M9 that can be continuously mapped by GEODAS data throughout the study area (i.e., over a strike distance > 450 km). M9 has also been mapped more than 100 km north of the study area to near 32.5°S by Schreckenberger et al. (2002). A broad trough east of M9 (solid black circle in Fig. 5), originally identified as M11 by Rabinowitz and LaBrecque (1979), can also be traced from line to line over the southern portion of the new survey (Fig. 3a and b). The horizontal separation of M9 and this trough is relatively consistent at roughly 60–70 km.

Our seafloor spreading model involves a uniform spreading rate of 28–30 mm/yr between M0 and M4 and a somewhat faster rate (40–44 mm/yr) for seafloor older than M4 (Fig. 6a). This change in rate is consistent with the earlier model of Rabinowitz and LaBrecque (1979), in that the pre-M4 observed anomalies are separated by greater distances than the corresponding features in their constant rate seafloor spreading model.

The regional lines show that between M9 and M11 the magnetic profiles display a series of small peaks superimposed upon a positive eastward slope (Fig. 5). We identify these as the peaks associated with several short normal polarity intervals within M10. These features, which are more clearly observed on Lines N37 and N38, correlate well with anomalies associated with M10Nn.1n, M10Nn.2n, and M10Nn.3n (Fig. 6b). Further north, on Line N5 and the regional GEODAS lines, these features appear less distinct but can still be followed from line to line. In particular the local minimum marked by the red arrow in Fig. 5 is interpreted as that due M10r. Because the distances between these various anomalies are consistent from line to line, the anomalies are interpreted as those produced by seafloor spreading.

The less well-defined character of the M10 to M11 anomalies over the northern part of the survey area may be attributed to the presence of abundant SDRs and associated interpreted magmatic underplating (Fig. 7a). SDRs appear to be absent south of the Cape Lineament (Koopmann et al., 2014b; Towle et al., 2015) where these M-series



**Fig. 6.** a – Correlations of observed magnetic anomaly profiles over the South African margin with proposed synthetic seafloor spreading model for M-series anomalies M0 to M11. Geomagnetic reversal time scale is from Gradstein et al. (2012). Magnetization of the oceanic crust =  $6 \text{ Am}^{-1}$ . Red arrow indicates a local minimum that is interpreted as M10r. b – Detailed correlations of observed magnetic anomaly profiles over the South African margin with proposed synthetic seafloor spreading model for M7r to “M11” anomalies. Magnetization of the oceanic crust =  $6 \text{ Am}^{-1}$ . c – Correlations of observed magnetic anomaly profiles over the South American margin with proposed synthetic seafloor spreading model for M-series anomalies M0 to M11. Profile A is Line BGR98-09 taken from Franke et al. (2010); Profile B is Line 3 taken from Becker et al. (2014). Note difference in amplitude scales for observed magnetic anomalies. Locations of profiles A and B shown in Fig. 8a. Magnetization of the oceanic crust =  $6 \text{ Am}^{-1}$ .

chrons are interpreted to be more fully developed. The ability of seafloor spreading magnetic anomalies to record short polarity intervals depends on a number of factors including depth to the magnetized layer, spreading rate, and the width of the intrusion/injection zone. The nearly constant separation of these major features suggests that there is no appreciable change in spreading rate between the northern and southern portions of the survey area. Anomaly amplitudes are somewhat larger in the north (Figs. 5 and 6a) suggesting shallower and/or thicker sources rather than deeper sources. The smoother nature of the anomalies north of the Cape Lineament is therefore attributed to a wider intrusion/injection zone, which is consistent with larger amounts of magmatic material reflected in the presence of abundant SDRs and associated underplating. The region immediately north of the Cape Lineament is described by Koopmann et al. (2014b) as a first order segment characterized by enormous SDR volumes.

We have constructed a seafloor spreading model for the South

American margin between  $44^{\circ}\text{S}$  and  $46^{\circ}\text{S}$  using magnetic profile data published by Franke et al. (2010) and Becker et al. (2012, 2014). The locations of these profiles are shown in Fig. 8a. The model, Fig. 6c, shows strong similarities to the model for the African margin. Specifically, the model has two spreading phases, one from M11 to ~M5, and a second from ~M5 to M0. The spreading rates for each phase are essentially the same as those for the African margin (43 mm/yr vs 44 mm/yr for the earlier phase, and 26 mm/yr vs 29 mm/yr for the later phase). Schreckenberger et al. (2002) identify anomaly M10 on the South American margin. We have extended this interpretation by identifying the magnetic low immediately west of M10 as anomaly M11 (Fig. 6c). The corresponding features are also observed on Line 3 from Becker et al. (2014), which is located immediately north of the FAFZ.

Landward of anomaly M11 on the African margin, we are able to correlate 2 additional magnetic features (G and H) over many of our profiles. Anomaly G is a magnetic minimum identified by Rabinowitz

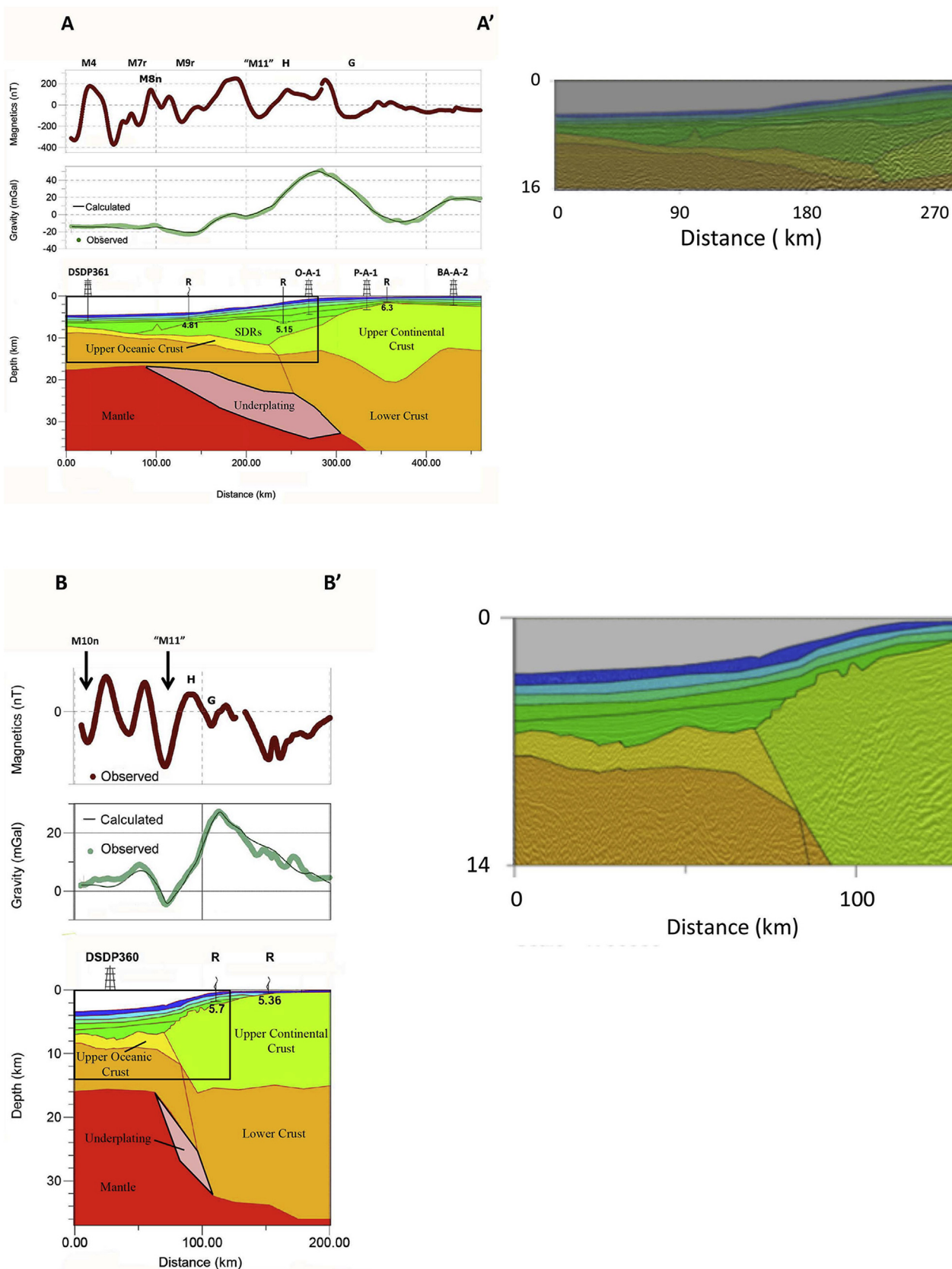


**Fig. 7.** Two-dimensional gravity models: a) A-A' and b) B-B'. Model locations are shown in Fig. 2 (with gravity anomalies), Fig. 3a (with chron identifications), and Fig. 3c (with magnetic anomalies). Each model includes four panels: 1) measured magnetic anomalies (red), 2) measured and calculated free air gravity anomalies (green and black respectively), 3) depth cross sections of modeled layers (see Table 2 for density values); which in-turn include, derrick symbols for wells along or near the models (showing deepest penetrations), "R" represents seismic refraction stations located along or near the models (km/s for deepest velocity annotations), and boxes outlining areas of the seismic reflection sections used for modeling, and 4) seismic reflection sections with colors from modeled layers.

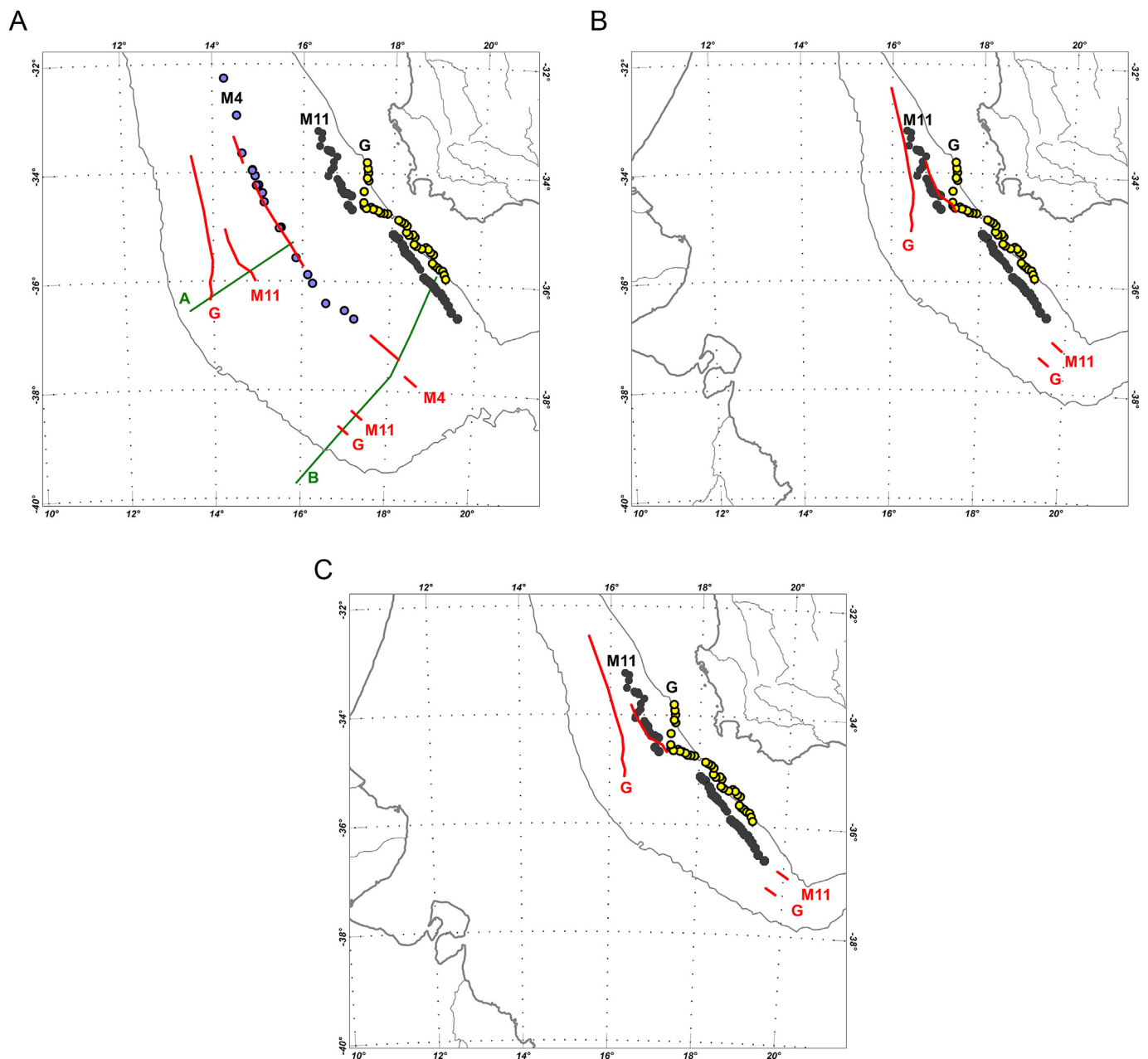


**Fig. 8.** Africa – South America coast line and 1 km isobath total reconstructions of the study area. a) M4 reconstruction: rotation angle and pole from Bird and Hall (2016), but the angle has been increased from  $54.038^\circ$  to  $54.2^\circ$  ( $+0.162^\circ$ ), South American magnetic anomaly profiles modeled in Fig. 6c (green), and the inset shows coast line and 1 km isobath reconstructions of the austral South Atlantic Ocean: Africa (green), South America M4 (blue) and South America M11 (red, Fig. 8c); b) M11 reconstruction: rotation angle has been increased to  $56.5^\circ$  using the same pole as M4 (Bird and Hall, 2016); and c) M11 reconstruction with a new pole:  $38.86^\circ\text{N}$ ,  $31.46^\circ\text{W}$  and  $56.6^\circ$  rotation angle. South American M4 lines are from Franke et al. (2007), Becker et al. (2012), and Koopmann et al. (2014a). South American M11 Chron and G-anomaly lines are from Koopmann et al. (2014a) in the north, and S.A. Hall in the south (this study). Africa M4 Chron, M11 Chron and G-anomaly picks are the same as Fig. 3.

and LaBrecque (1979) that they were able to map over large distances along both the African and South American margin. Anomaly H (Fig. 3) is a magnetic maximum that can also be traced on several of our profiles. The location of this anomaly varies along strike, separated from M11 by distances that vary from less than 10 km to more than 40 km. For this reason, we do not consider anomaly H to be a seafloor spreading anomaly.

#### 4.2. Discontinuities and possible fracture zones

Discontinuities involving offsets of seafloor spreading magnetic lineations are commonly associated with fracture zones and transform

faults. However, such discontinuities are not necessarily evidence of transform motion or of the existence of fracture zones. As pointed out by Taylor et al. (2009) and Gerya (2013a, b) some initial spreading offsets may simply reflect initial en-echelon rift geometry. Other offsets may be pseudofaults oblique to the spreading direction that are produced by rift propagation (Hey, 1977; Hey et al., 1980). Some of the discontinuities mapped here correspond to fracture zones previously proposed based upon sparse regional magnetic coverage (Bolli et al., 1978; Rabinowitz and LaBrecque, 1979).

Discontinuity D1 (Fig. 3a) offsets only a few magnetic anomalies and does not appear to extend significantly seaward of the new survey area. It coincides with an unnamed fracture zone south of the Titiesbaai

FZ (Bolli et al., 1978) at which a right lateral offset was previously mapped. The seaward reduction in offset from ~30 km for the magnetic minimum interpreted as M11 to essentially zero for M7 may be associated with asymmetric spreading or a change in spreading direction. Anomaly M11 has an azimuth of N 35–40° W whereas M7 trends N 25–30° W. The orientation of this discontinuity (~N65°E) is in good agreement with fracture zone azimuths of N60° ± 5° predicted by published poles of rotation for M0 to M4 time. (Nürnberg and Müller, 1991; Torsvik et al., 2009; Moulin et al., 2010; Heine et al., 2013; Bird and Hall, 2016).

At discontinuity D2 there is a major break in the continuity of all features mapped in the new survey but none of the M-series anomalies (M9, M7, M4 etc.) appear to undergo any significant offset across this discontinuity (Fig. 3c). D2 coincides approximately with a small change in orientation of M4 and M0 isochrons from ~N40°W southeast of 36°S to N30°W to the northwest (Müller et al., 1997). Discontinuity D2 also coincides with the Cape Segment Boundary of Koopmann et al. (2014b) and the Cape Lineament of Towle et al. (2015), which appears to represent a major change in crustal structure. The dominant magnetic low associated with discontinuity D2 trends N 35° E, similar to the trend of discontinuity D3 and possibly that of D4 but different to the azimuth predicted by published poles of rotation for M4 (Nürnberg and Müller, 1991; Torsvik et al., 2009; Moulin et al., 2010; Bird and Hall, 2016) and the observed trend of the nearby Agulhas FZ. It appears that discontinuity D2 may mark a major crustal boundary at the Cape Lineament, rather than a fracture zone.

Discontinuities D3 and D4 have similar orientations, can be traced over more than 100 km and involve offsets of younger (e.g., M7, and M4) magnetic anomalies and therefore appear more likely to be produced by fracture zones. As noted by Rabinowitz (1976), discontinuity D3 is not parallel to the nearby FAFZ but trends in a more northerly direction (Fig. 2). Discontinuity D3 orientation (~N35°E) is also not orthogonal to the trend of the magnetic lineations (40°W) nor consistent with flowline directions predicted by most poles of rotation for Southern Africa and South America for M4 time. It is possible that this more northerly orientation reflects a more oblique direction of plate motion during the earliest phase of spreading between 130 and 135 Ma as suggested by other authors (e.g., Franke, 2013). Alternatively, it may reflect motion involving deep crustal blocks of the CFB during the earliest phase of opening. In this model, the deep-seated “Cape Syntaxis” (Figs. 2 and 3) (Johnston, 2000), which marks the intersection of the E-W trending Permo-Triassic CFB and the N-NW-S-SE trending Gondwana Gariep Fold Belt (Paton et al., 2017a), may have provided an inherited structural fabric along which the strike of later Jurassic and early Cretaceous rifting took advantage. It is possible that the oblique trend of discontinuity D3 relative to the strike of the FAFZ is an inherited trend from the deeper CFB and Gariep Fold Belt intersection, which extends offshore.

#### 4.3. Crustal structure of the African margin north of the Cape Lineament

On both the South American and African margins a magnetic anomaly, designated as “G” by Rabinowitz and LaBrecque (1979), is observed to more or less coincide with the landward limit of SDRs (Koopmann et al., 2014a). Crustal profiles of the African margin between the Walvis Ridge and the Cape Lineament based upon deep penetration seismic data include both SDRs in the near surface, and a lower crustal layer characterized by higher than normal P-wave velocity ( $V_p \sim 7.1$  to 7.6 Km/s). This lower layer has been interpreted as evidence of magmatic underplating (Bauer et al., 2000; Gladchenko et al., 1998; Hirsch et al., 2009; Becker et al., 2014). The location of the underplating with respect to the overlying SDRs appears to vary along strike beneath both margins (Becker et al., 2014) but immediately north of the study area, seismic data (Hirsch et al., 2009; Becker et al., 2014) show an approximate spatial correspondence between the horizontal extent of SDRs observed in the near surface layers and the location of

the lower crustal body such that the underplating is located directly beneath the SDRs.

The Springbok line, a wide-angle seismic reflection/refraction profile near 31°S, crosses a portion of the Orange Basin where Rabinowitz and LaBrecque (1979) mapped M-series anomalies M4 to M11 and anomaly G. Correlation of M7 and M9, as identified by Rabinowitz and LaBrecque (1979), with the crustal structure indicates that they are located over underplated crust interpreted as transitional by Hirsch et al. (2009). Anomaly G is located over the boundary between transitional and intruded continental crust. Within the new survey area, seismic studies have mapped a broad region of SDRs (Koopmann et al., 2014b; Towle et al., 2015) north of the Cape Lineament but none has mapped the deep crust/Moho boundary and consequently the nature of the deep crust is unknown. In their study, Koopmann et al. (2014b) identify distinct SDR wedges (Fig. 3a) over the region where we interpret M-series anomalies M7 to M11. In particular, over the northernmost part of the study area, anomaly M7 is located just seaward of the western edge of the SDRs (Koopmann et al., 2014b) but both M9 (located between SDR wedge 4 and wedge 3), and M11 (located close to the boundary between wedges 2 and 3) are over crust we interpret in our gravity models as thickened by underplating. The inner set of SDRs (wedge 1) is mapped approximately 70 km landward of our M11 pick. In the central part of our study area, just north of the Cape Lineament, anomaly M9 is again located between SDR wedge 4 and wedge 3. Based upon our interpretation of the magnetic anomaly data, some seafloor spreading anomalies are produced by crust that is covered by SDRs but a portion of the SDR-covered areas (wedge 1 and parts of wedge 2) is underlain by crust that does not produce clearly identifiable seafloor spreading anomalies.

In the case of the Springbok line (Hirsch et al., 2009), anomaly G coincides with both the landward limit of SDRs and the landward extent of the underplating. This correspondence may apply further south in the northern portion of our study area (i.e., north of the Cape Lineament) such that the spatial distribution of the SDRs provided by seismic data from this study, and Koopmann et al. (2014b), and the location of the G anomaly may indicate an approximate location for the landward limit of the lower, underplating crustal layer. Our crustal model, profile A-A' (Fig. 7a), shows a ~220 km wide region of underplated crust that extends from magnetic anomaly G seaward to near M8n, which is located over normal thickness oceanic crust (Fig. 7a). Anomalies M9 to M11 are located over a region of underplated crust that is ~13–18 km thick. Landward of M11 is a ~70–80 km wide region of underplated crust that corresponds to the inner SDR wedges 1 and 2 of Koopmann et al. (2014b) but is not associated with seafloor spreading anomalies. Well Soekor O-A1/Z1 was drilled in this location and penetrated 200 m of vesicular, amygdaloidal basalts and interbedded sediments interpreted to be subaerially extruded lava fields (SDRs). We therefore interpret this region of underplated crust to be a transition zone from stretched continental crust with substantial magmatic intrusions (perhaps a zone of “overplated” sills or SDRs fed by a thick underplated magma chamber) to a thickened, completely intruded oceanic crust that progressively thins to more normal thickness oceanic crust at its seaward edge.

#### 4.4. Crustal structure of the African margin south of the Cape Lineament

South of the Cape Lineament, SDRs are either absent or poorly developed (Koopmann et al., 2014b; Towle et al., 2015), and magnetic anomaly G is not well defined (Rabinowitz and LaBrecque, 1979). Consequently, our initial crustal model for this area did not include underplating. However, recent crustal modeling of the conjugate South American margin, south of the Colorado Transfer Zone, by Becker et al. (2014) based upon seismic refraction data indicates the presence of a small amount of underplating in an area where there is little or no evidence of SDRs. Our final crustal model south of the Cape Lineament, profile B-B', therefore includes a thin (< 5 km) lower crustal layer

(Fig. 7b). Anomalies M7, M9, M10n and M10Nn.3n are all observed over normal thickness oceanic crust and seaward of a major change in slope of the basement surface displayed on the southernmost profile of Koopmann et al. (2014b). Gravity model B-B' (Fig. 7b) indicates a narrow (~35 km wide) region of crustal thinning associated with continental rifting. Well Soekor C-B1 drilled approximately 20 m of biotite schist and quartzite at 1851 m subsea true vertical depth and provides a point of control for the probable seaward extent of continental crust (Fig. 2). Landward of M11 the basement changes slope abruptly from shallow to very steep (Koopmann et al., 2014b) and the crust appears to thicken rapidly to the east (Fig. 7b). We interpret the 35–40 km wide zone between our oldest M-series anomaly and full continental thickness to represent the ocean-continent transition zone (Fig. 7b). We associate this change in slope as defining the seaward boundary of the zone of stretched continental crust.

#### 4.5. Reconstructions

We have reconstructed the positions of those portions of the African and South American margins south of 32°S at the time of M4 (i.e., ~131 Ma) (Fig. 8a). We used the M4 rotation pole of Bird and Hall (2016) with a slightly larger rotation angle (viz 54.2°) than that published previously. The fit of the M4 isochrons from the conjugate margins is excellent.

Using the same M4 pole, we attempted to reconstruct the margins for “M11” time. Using a rotation angle of 56.5°, we were able to obtain a satisfactory fit for the M11 isochrons in the northern part of our study area but a significant gap remained for the isochrons in the south (Fig. 8b). Closing this gap using our M4 pole and a larger rotation angle produced a significant overlap of the isochrons further north. To overcome this problem, we have calculated a new pole for our M11 isochrons. This pole is located at 38.86°N, 31.46°W (Table 3) approximately 7° south of our M4 pole. As shown in Fig. 8c, a rotation of 56.6° about this pole results in a good fit of the M11 isochrons from both margins. This pole applies only to the southernmost margins of the Austral segment where M11 is observed and is used here to document the portions of the margin where crustal separation has taken place and new oceanic lithosphere created. At this time further north, the margins are undergoing non rigid deformation that includes both crustal extension and magmatic underplating.

## 5. Discussion

### 5.1. Anomaly G and crustal boundaries

Anomaly G north of the Cape Lineament has a similar amplitude (~330–500 nT) and wavelength (peak to trough distance ~60–80 km) to the East Coast Magnetic Anomaly (ECMA) (Taylor et al., 1968;

**Table 1**

Key to correlated magnetic anomalies shown as color filled circles in Fig. 3a. Colors correspond to interpreted M-series seafloor spreading magnetic anomalies. Ages are based on the time scale of Gradstein et al. (2012).

Chron	Color	Age (Ma)
M0r	yellow, outboard	125.93
M2 (M3n)	red, outboard	128.66
M4 (M5n)	light blue	130.60
M7r	orange	132.27
M9r	purple	133.30
M10N.1n	pink	134.22
M10Nn.1r	green	134.48
M10Nn.3n	brown	134.78
M11n	red, inboard	135.32
M11r.1r	black	135.92
"H"	dark blue	
"G"	yellow, inboard	

**Table 2**

Densities assigned to the layers used in the gravity models shown in Fig. 7.

Layer	Density (gm cm <sup>-3</sup> )
Sedimentary 1	2.15
Sedimentary 2	2.27
Sedimentary 3	2.42
Sedimentary 4	2.53
Sedimentary 5	2.55
SDR	2.65
Upper oceanic crust	2.80
Upper continental crust	2.70
Lower crust	2.90
Underplating	3.10
Mantle	3.20

**Table 3**

Total reconstruction poles for the South Atlantic Ocean from previous workers and this study. Their locations are displayed in Fig. 9.

Chron	Age (Ma)	Lat.(°)	Long.(°)	Rotation(°)	Source
C5	9.8	72.4	-49.7	4.3	Bird and Hall, 2016
C5	9.8	54.1	-34.8	3.2	Perez-Diaz and Eagles, 2014
C5	9.8	59.5	-39.6	3.1	Nankivell, 1997
C5	9.8	60.0	-39.0	3.2	Cande et al., 1988
C5	9.8	57.4	-37.5	3.7	Pindell and Dewey, 1982
C24	52.6	57.7	-30.4	22.4	Bird and Hall, 2016
C24	52.6	61.3	-32.1	21.2	Perez-Diaz and Eagles, 2014
C24	52.6	61.9	-32.3	21.2	Nankivell, 1997
C24	52.6	60.0	-32.0	21.2	Cande et al., 1988
C22	48.6	60.8	-36.6	21.3	Pindell and Dewey, 1982
C25	57.1	63.0	-36.0	22.8	LaBrecque and Hayes, 1979
C34	83.6	59.4	-34.2	33.6	Bird and Hall, 2016
C34	83.6	60.7	-33.9	33.4	Perez-Diaz and Eagles, 2014
C34	83.6	59.0	-37.0	41.3	Eagles, 2007
C34	83.6	61.9	-34.3	33.5	Nankivell, 1997
C33r	79.9	63.0	-34.0	31.0	Nürnberg and Muller, 1991
C34	83.6	61.8	-34.0	33.5	Cande et al., 1988
C34	83.6	63.0	-36.0	33.8	Pindell and Dewey, 1982
C34	83.6	63.0	-36.6	33.8	LaBrecque and Hayes, 1979
C34	83.6	63.0	-36.0	33.8	Rabinowitz and LaBrecque, 1979
M0	125.9	43.4	-32.2	52.2	Bird and Hall, 2016
M0	125.9	57.4	-39.9	53.5	Perez-Diaz and Eagles, 2014
M0	125.9	56.8	-37.9	53.7	Eagles, 2007
M0	125.9	51.6	-35.0	52.9	Nürnberg and Muller, 1991
M0	125.9	55.1	-35.7	50.9	Pindell and Dewey, 1982
M4	130.6	45.5	-33.0	54.0	Bird and Hall, 2016
M5n	130.6	57.4	-40.0	55.9	Perez-Diaz and Eagles, 2014
M5n	130.6	56.5	-38.4	55.6	Eagles, 2007
M4	130.6	50.4	-33.5	54.4	Nürnberg and Muller, 1991
M4	130.6	55.1	-35.7	49.4	Curie, 1984
M11	136.1	38.9	-31.5	56.7	Hall et al., this study
M11	136.1	56.3	-38.8	57.5	Eagles, 2007
M11	136.1	47.0	-33.8	58.0	Vink, 1982

Behrendt and Klitgord, 1980; Alsop and Talwani, 1984; Bird et al., 2007), and similar anomalies over other continental margins, which have also been associated with SDRs (Dehler et al., 2004). Comparison of the crustal profiles over the African margin based upon deep penetration seismic data with magnetic data indicates that the “G” anomaly of Rabinowitz and LaBrecque (1979) is closely associated with the landward limit of the underplated layer. Various magnetic models have been proposed to explain the ECMA including recent simple 2-D models that assign a magnetization of ~6 A/m to a single SDR source body located over the seaward end of thinned continental crust (Dehler, 2012). This value is similar to that used by Talwani and Abreu (2000) for their source of the ECMA and corresponds well with values of 4–6 A/m used in SDR modeling studies of the Norwegian margin (Schreckenberger et al., 1997) and Argentine margin (Hinz et al., 1999). Similar magnetizations for SDRs along the African margin have

been used by Corner et al. (2002). However, the presence of the G anomaly south of the Cape Lineament, albeit reduced in amplitude (Rabinowitz and LaBrecque, 1979), in a region where SDRs are not imaged seismically suggests that SDRs alone are insufficient to generate the anomaly. This is similar to the Scotian margin where the ECMA extends eastward with reduced amplitude in a region where SDRs have not been observed (Dehler, 2012; Keen and Potter, 1995), and to the South America margin south of the Colorado Transfer where a weak G anomaly is observed (Rabinowitz and LaBrecque, 1979) but SDRs have not been mapped. Our interpretation of this is that the SDRs together with the associated intrusions and the lower crustal body are responsible for generating anomaly G. This is not consistent with models proposed by Dehler (2012) for the ECMA in which the SDRs are entirely responsible for observed anomaly amplitude. Dehler (2012) explains the ECMA over the eastern Scotian margin by proposing that SDRs are present but undetected with available data. We propose that south of the Cape Lineament, anomaly G may be produced by limited intrusives and the underplating layer. Overall, we identify the G anomaly as defining a change in crustal structure from continental to transitional crust at volcanic margins. The larger distance between anomaly G and M11 north of the Cape Lineament, as shown in Fig. 3a, is consistent with a broad zone of thick, magmatically underplated crust.

### 5.2. Seafloor spreading and underplated crust

Seafloor spreading anomalies have been mapped elsewhere over regions where SDRs and underplated crust are observed including along the Norwegian margin (Tsikalas et al., 2002; Breivik et al., 2009), the Gascoyne margin of western Australia (Rey et al., 2008), and the Jan Mayen Ridge (Breivik et al., 2012). Much of this crust appears to have a greater affinity with oceanic crust than continental crust, and we therefore interpret crust seaward of our M11 anomaly as a thick oceanic crust that must be removed in any pre-drift fit of Africa and South America. The nature of the crust in the region between M11 and anomaly G – a distance of ~75 Km on profile 24 (Fig. 5) – is unknown but likely is stretched and substantially intruded continental crust.

The distance between the well-defined magnetic isochron M4 and anomaly G decreases significantly along strike from ~230 km near 34°S where we identify M11 to less than 160 km just south of the Walvis Ridge, where only M4 can be reliably identified (Rabinowitz and LaBrecque, 1979). The width of the underplated region also varies along strike from ~220 Km near 31°S (Hirsch et al., 2009) to 150 to 160 Km near 23°S where M4 is identified within the region of underplated crust (Bauer et al., 2000). Becker et al. (2014) have examined variations in the location and horizontal extent of SDRs and those of the underlying underplated region along each margin of the South Atlantic. These authors found that towards the northern end of the Austral segment (i.e., near the Rio Grande/Walvis Ridge) the underplated region extends seaward of the SDRs, whereas towards the southern end (i.e., near the FAFZ), the underplated region is smaller and thinner and is not overlain by SDRs. Over the central portion of the margin, just north of our study area, the underplated region has approximately the same width and horizontal position as the overlying SDRs.

Our results and those of others suggest a model for the evolution of the margin that begins with a period of continental extension/rifting during which magmatic material pools at the base of an attenuated continental crust and through a non-systematic, disorganized dike injection process produces SDR flows at the surface. This crust is similar in nature to the crust beneath the inner SDRs in Argentina proposed by Franke et al. (2010). Continued crustal extension further weakens the crust and begins to focus dike injection into a narrower region. Ultimately, prolific dike injection results in a single, wide injection zone and the continental crust is entirely severed. At this time, the process of further dike injection becomes synonymous with formation of new oceanic crust and the beginning of seafloor spreading albeit with a thicker than normal crust. Slow continental extension is replaced by

more rapid seafloor spreading which results in a gradual thinning of the new oceanic crust. This model is similar to that originally described by Franke et al. (2010) and more recently proposed for the South American margin by Paton et al. (2017b).

In this model, overlapping SDRs over the attenuated/rifted continent and their associated non-systematic distribution of dikes produce isolated magnetic anomalies rather than a linear pattern of magnetic stripes. It is only when the single, wide intrusion zone is formed that magnetic anomalies produced by the magnetized dikes develop into seafloor spreading anomalies. One implication of this model is that continental extension and SDR formation may be active at one part of the margin at the same time that seafloor spreading has already begun at another part of the margin.

The mode of formation of SDRs and their relationship, if any, to underplating is a topic of active debate. Recently a numerical model developed to explain SDR geometry and their development through time (Buck, 2017) explores the effects of loading subsidence produced by the SDR flows rather than continental rifting. In this model, sequences of individual SDR wedges are produced by jumps in the location of the dike injection zone and/or periods of quiescence when no flows are produced. The model does not include any influence from the underplating and so its role in the development of SDRs remains unclear.

### 5.3. Change in crustal character across the Cape Lineament

These two sectors, the southern Orange Basin and the Cape Basin, are separated by a regional NE-SW trending structural ridge or discontinuity, which we have termed the “Cape Lineament”. The Cape Lineament appears to have acted as a physical barrier during the initial stages of basin formation with early volcanism related to seafloor spreading possibly taking place in a marine environment to the south and subaerially to the north.

Figs. 3a and 7a show that north of the Cape Lineament anomaly M9 is reliably identified within the region covered by SDRs (Koopmann et al., 2014b; Towle et al., 2015). Whereas south of the Lineament, M9 is also reliably identified but is located in an area where SDRs are either absent or only very weakly developed (Fig. 7b). Thus, while the nature of the crust appears to differ north and south of the Lineament, seafloor spreading anomalies appear to continue across this boundary. In a similar way, M4 is located seaward of the underplated zone in our study area but is located within the underplated zone further north (Bauer et al., 2000). The implication is that while the thickness of the crust varies along strike, the mode of emplacement remains similar i.e., by intrusion of new oceanic material at a spreading center.

The change in crustal character in crossing the Cape Lineament also appears to be reflected in the thickness of sedimentary layers. North of the Lineament total sedimentary thickness is less than 3 km whereas to the south, sedimentary layers are almost 5 km thick (Fig. 4). The presence and the curvilinear strike of the CFB onshore, which approximately lines up with the strike of the Cape Lineament offshore, appears to have precluded the development of major Cretaceous drainage systems to the study area. This is in stark contrast to the abundance of Cretaceous sedimentation preserved in the northern Orange Basin (up to 8 km), derived from the Olifants and Orange River systems (Jungslager, 1999; Van der Spuy, 2003; Kounov et al., 2008), and the uplift, exhumation, and pattern of Cretaceous sedimentation in the Bredasdorp and Outeniqua basins to the east of Cape Agulhas (Van der Spuy, 2003; Tinker et al., 2008) derived from smaller river systems. Thus, variations in the amount of coeval sediment supply are not believed to be a significant factor in sediment thickness along this part of the margin. Instead, differences in sediment thickness across the Cape Lineament are probably due to variations in accommodation space and are more likely the result of variations in subsidence related to crustal thickness rather than loading due to variations in sediment supply. This implies a somewhat thicker crust beneath the region north of the

Lineament consistent with the widespread presence of SDRs and evidence of underplating further north (Springbok line) (Hirsch et al., 2009).

#### 5.4. Comparison with South American margin

M-series anomalies M2 to M10 have been observed over the South American margin near 44°S (Schreckenberger et al., 2002). Spreading rates for these anomalies are slightly less than those over the African margin but display a similar pattern with a faster spreading rate of ~43 mm/yr between M11 and M4/M5 and slower rates of approximately 26 mm/yr between M4/M5 and M0 (Fig. 6c). Poles of rotation that reconstruct the South Atlantic at M4 time (Nürnberg and Müller, 1991; Torsvik et al., 2009; Moulin et al., 2010; Heine et al., 2013; Bird and Hall, 2016) juxtapose our survey area adjacent to the South American area shown in Schreckenberger et al. (2002). Our survey has a greater latitudinal range than that of Koopmann et al. (2014b) allowing us to map pre-M5 anomalies further south along the African margin.

#### 5.5. Reconstruction

Many previous reconstructions of the South Atlantic considered only rigid plate behavior. As a result, to explain the diachronous opening produced by the northward progression of seafloor spreading, several authors have proposed models that involve deformation along various intraplate tectonic zones and/or corresponding motions along continental strike slip or transfer faults (e.g., Curie, 1984; Unternehr et al., 1988; Nürnberg and Müller, 1991; Eyles and Eyles, 1993; König and Jokat, 2006; Eagles, 2007; Moulin et al., 2010; Torsvik et al., 2009; Perez-Diaz and Eagles, 2014). These intra-plate boundaries and the motion along them are inferred to be active prior to M4 time. In our model for the development of the South Atlantic, we suggest that much of this motion may be unnecessary as the seafloor spreading in the southernmost part of the basin is accommodated further north by non-rigid behavior associated with extension of the lithosphere and magmatic underplating. Several authors have discussed how extension rates associated with continental rifting do not match seafloor spreading rates and have proposed various non-rigid mechanisms to account for this including weak coupling of the crustal and mantle portions of the lithosphere (e.g., Kington and Goodliffe, 2008; Liao and Gerya, 2015).

With a northward progression of seafloor spreading through time, more of the margins act in a rigid fashion and the motion associated with seafloor spreading can be described by a pole of rotation. Such poles, however, do not describe motions involving the entire African and South American plates, as crustal separation has not occurred along the entire plate boundary. Published rotation poles for various times from M11 (this study) through C24 appear to form a generally northward progression along an azimuth of roughly N10°W consistent with the corresponding northward initiation of seafloor spreading (Fig. 9). Similar models for the zipper-like opening of ocean basins by progressive tearing of the continental lithosphere have been proposed for other areas including the Gulf of Aden (Courtilot, 1980; Brune and Autin, 2013), the Woodlark Basin (Taylor et al., 1999), the Afar (Bastow and Keir, 2011) and the Laptev Sea (Engen et al., 2003).

## 6. Conclusions

Newly acquired, high quality, marine, total field magnetic data over the Atlantic margin of South Africa display a series of well-defined linear magnetic anomalies oriented sub-parallel to the coast that we interpret as M-series seafloor spreading anomalies. We have identified the earliest continuous lineation as that produced by magnetochron M10Nr (named “M11” in earlier studies) suggesting that the drift stage of continental separation developed around 135 Ma (Late Valanginian/Early Hauterivian) in this part of the South Atlantic Basin. We identify

M11 throughout the new survey area between 33° S and 36.5° S but with greater confidence over the southern portion (i.e., south of 34.5° S). Seafloor models for the M-series anomalies suggest a 2-stage spreading history: a more rapid (44 mm/yr) initial spreading phase between M11 and M4/M5 followed by slower (29 mm/yr) spreading from M4/M5 to M0. Corresponding anomalies identified on the conjugate South American margin north of the FAFZ are consistent with a similar 2-stage development.

The pattern of linear features is interrupted in several places by roughly northeasterly trending discontinuities that offset some but not all of the M-series anomalies. One of these discontinuities, herein called the Cape Lineament, crosses the survey area in a roughly NE-SW direction separating two distinct crustal types: SDR-covered, thick oceanic crust to the north, and to the south a more normal thickness oceanic crust where SDRs are either absent or have much more limited areal extent.

A distinctive magnetic anomaly, Anomaly G, identified in previous studies is observed over both margins and corresponds approximately with the landward limits of both the SDRs and, where observed, crustal underplating. The distance between anomaly G and M11 in our study area varies along strike. South of the Cape Lineament anomaly G is located 35–40 km landward of M11 but north of the Lineament the anomaly G – M11 distance is 80–90 km. The nature of the crust between M11 and anomaly G is unknown but here is interpreted as extensively intruded, attenuated continental crust. The larger distance between anomaly G and M11 north of the Cape Lineament is consistent with the more magmatic nature of the crust in this area.

We have reconstructed the locations of the conjugate margins for the Austral portion of the South Atlantic south of 32°S for both M4 and M11 times. To obtain a satisfactory fit of the M11 isochrons we have calculated a new rotation pole at 38.86°N; 31.46°W.

## Acknowledgements

The authors wish to thank Anadarko Petroleum Corporation for granting permission to publish these data and interpretations. Marek Ranzoszek of Anadarko South Africa Pty. enabled local oversight during 2D seismic, gravity and magnetic data acquisition in 2012–13 from Cape Town. David van der Spuy and Viljoen Storm of the Petroleum Agency of South Africa provided technical and logistical support. Answa De Lange and Noluthando Jukuda of PetroSA were gracious with their time and ideas. We are grateful to PGS (UK) for allowing the publication of the seismic data presented in Fig. 4. Ophelia Kersten of Anadarko Petroleum Corporation provided valuable assistance with the figures. Critiques by two anonymous reviewers substantially improved the content of the manuscript.

## Appendix A. Supplementary data

Supplementary data related to this article can be found at <http://dx.doi.org/10.1016/j.marpetgeo.2018.03.010>.

Elements that are common in Figs. 2 and 3: Two-dimensional modeled cross sections (Fig. 7) are heavy red lines; inboard and outboard blue and white circles posted on the model lines correspond to the extents of modeled magmatic underplating, and blue and green circles correspond to the modeled boundary between oceanic and continental crust; line numbers for marine tracklines correspond to profiles displayed in Fig. 5: “G” for GEODAS and RL24, which is heavier, for Rabinowitz and LaBrecque (1979) profile 24; interpreted discontinuities are heavy dashed lines (D1 through D4); new high-resolution marine magnetic data survey outline (dashed black or thick white); geomagnetic isochrons (Müller et al., 1997) dotted black lines; bathymetry contour interval is 1 km (blue); onshore outcropping basement areas are colored black; the north-south and east-west oriented lines over South Africa trace the Cape Syntaxis (modified after Koopmann et al., 2014b).

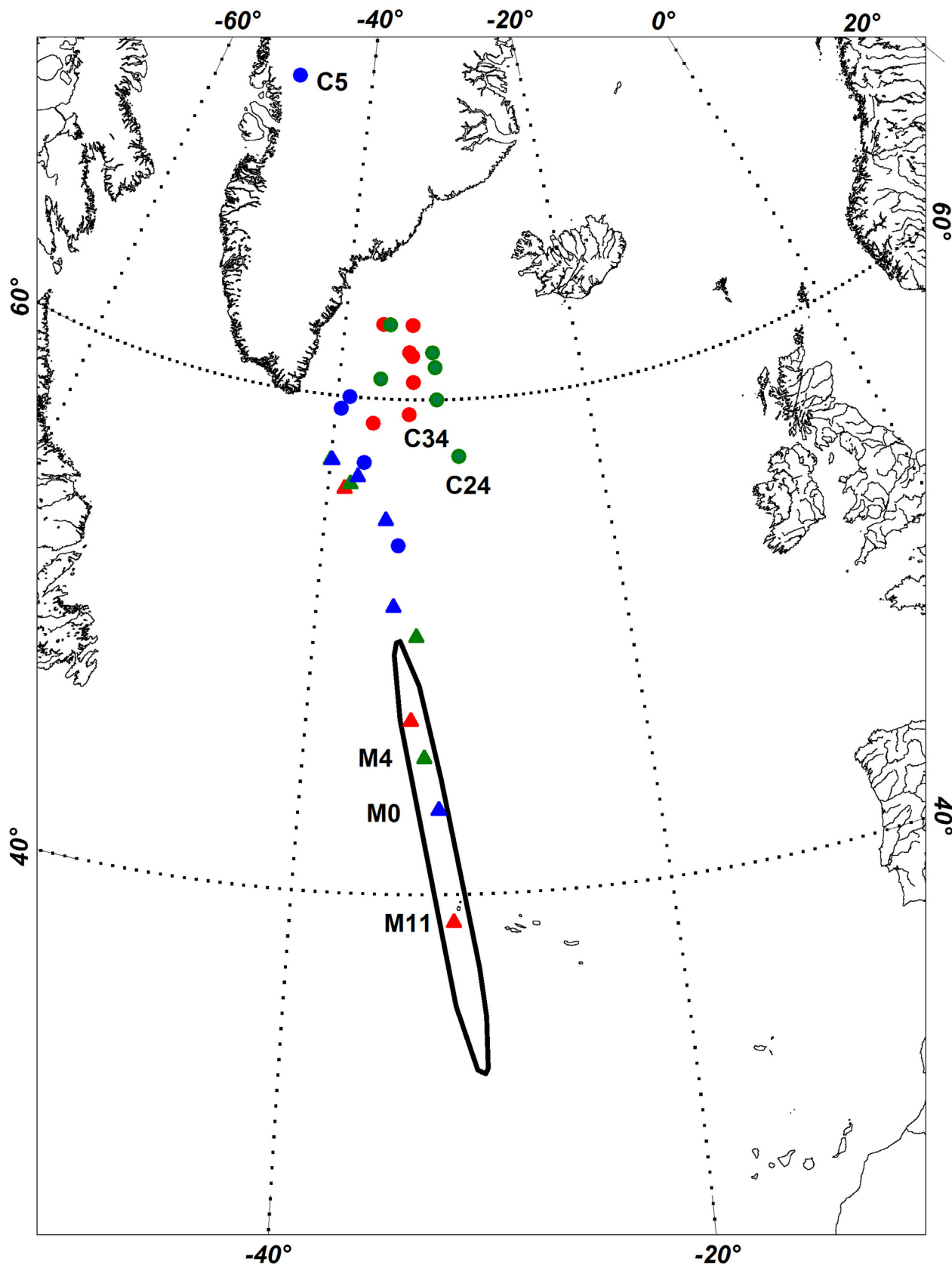


Fig. 9. –Total reconstruction poles from this study and previous studies (see Table 3 for sources). Error ellipsoid calculated for M11 (this study) is the 90% confidence region. Cenozoic poles are color-filled circles: C5 (blue), C24-group (green, C22, C24 and C25) and C34 (red). Mesozoic poles are color-filled triangles: M0 (blue), M4 (green) and M11 (red). Labelled chrons are those from Bird and Hall (2016) and this study, and the coordinate system is UTM 25 North, WGS84.

## References

- Alsop, L.E., Talwani, M., 1984. The east coast magnetic anomaly. *Science* 226, 1189–1191.
- Bastow, I.D., Keir, D., 2011. The protracted development of the continent-ocean transition in Afar. *Nat. Geosci. Lett.* <http://dx.doi.org/10.1038/NNGEO1095>. March.
- Bauer, K., Neben, S., Schreckenberger, B., Emmerman, R., Hinz, K., Jokat, W., Schulze, A., Trumbull, R.B., Weber, K., 2000. Deep structure of the Namibia continental margin as derived from integrated geophysical studies. *J. Geophys. Res.* 105, 25829–25853.
- Becker, K., Franke, D., Schnabel, M., Schreckenberger, B., Heyde, I., Krawczyk, C.M., 2012. The crustal structure of the southern Argentine margin. *Geophys. J. Int.* 189, 1483–1504.
- Becker, K., Franke, D., Trumbull, R., Schnabel, M., Heyde, I., Schreckenberger, B., Koopmann, H., Bauer, K., Jokat, W., Krawczyk, C.M., 2014. Asymmetry of high-velocity lower crust on the South Atlantic rifted margins and implications for the interplay of magmatism and tectonics in continental breakup. *Solid Earth* 5, 1011–1026.
- Behrendt, J.C., Klitgord, K.D., 1980. High-sensitivity aeromagnetic survey of the U.S. Atlantic continental margin. *Geophysics* 45, 1813–1846.
- Bird, D.E., Hall, S.A., 2016. Early seafloor spreading in the south Atlantic: new evidence for m-series magnetochrons north of the Rio Grande fracture zone. *Geophys. J. Int.* 206, 835–844.
- Bird, D.E., Hall, S.A., 2010. Early seafloor spreading in the south Atlantic Ocean: m-series isochrons north of the Rio Grande fracture zone? In: (abstract): 2nd Conjugate Margins Conference, Lisbon, Portugal.
- Bird, D.E., Hall, S.A., Burke, K., Casey, J.F., Sawyer, D.S., 2007. Early central Atlantic Ocean seafloor spreading history. *Geosphere* 3 (5), 282–298.
- Bolli, H.M., Ryan, W.B.F., Foresman, J.B., Hottman, W.E., Kagami, H., Longoria, J.F., McKnight, B.K., Melguen, M., Natland, J.H., Proto-Decima, F., Siesser, W.G., 1978. Cape Basin continental rise: sites 360 and 361. In: Bolli, H.M., Ryan, W.B.F. (Eds.), *Init. Repts. DSDP*, vol. 40. U.S. Govt. Printing Office, Washington, pp. 29–182.
- Breivik, A.J., Faleide, J.I., Mjelde, R., Flueh, E.R., 2009. Magma productivity and early seafloor spreading rate correlation on the northern Voring margin, Norway – constraints on mantle melting. *Tectonophysics* 468, 206–223.
- Breivik, A.J., Mjelde, R., Faleide, J.I., Murai, Y., 2012. The eastern Jan Mayen micro-continent volcanic margin. *Geophys. J. Int.* 188, 798–818.
- Brune, S., Autin, J., 2013. The rift to break-up evolution of the Gulf of Aden: insights from 3d numerical lithospheric-scale modelling. *Tectonophysics* 607, 65–79.
- Buck, W.R., 2017. The role of magmatic loads and rift jumps in generating seaward dipping reflectors on volcanic margins. *Earth Planet Sci. Lett.* 466, 62–69.
- Cande, S.C., Rabinowitz, P.D., 1978. Mesozoic seafloor spreading bordering conjugate continental margins of Angola and Brazil. In: 10<sup>th</sup> Annual Offshore Technology Conference, vol. 3268. OTC, Houston, Tex, pp. 1869–1876 May 8–11.
- Cande, S.C., LaBrecque, J.L., Haxby, W.F., 1988. Plate kinematics of the south Atlantic: chron 34 to present. *J. Geophys. Res.* 93, 13479–13492.
- Channell, J.E.T., Erba, E., Nakanishi, M., Tamaki, K., 1995. Late Jurassic-Early Cretaceous time scales and oceanic magnetic anomaly block models. *SEPM Special Publication No. 54* In: Berggren, W.A. (Ed.), *Geochronology, Time Scales and Global Stratigraphic Correlation*. Soc. Econ. Min. Pet. pp. 51–63 Tulsa, OK.
- Corner, B., Cartwright, J., Swart, R., 2002. Volcanic passive margin of Namibia: a potential fields perspective. *Geol. Soc. Am. Spec. Pap.* 362 293–220.
- Courtillot, V.E., 1980. Opening of the Gulf of Aden and Afar by progressive tearing. *Phys. Earth Planet. Int.* 21, 343–350.
- Curie, D., 1984. Ouverture de l'Atlantique sud et discontinuités intra-plaques: une nouvelle analyse. *Univ. de Bretagne Occidentale, Brest*, pp. 192.
- Dehler, S.A., 2012. Initial rifting and breakup between Nova Scotia and Morocco: insight from new magnetic models. *Can. J. Earth Sci.* 49, 1385–1394.
- Dehler, S.A., Keen, C.E., Funck, T., Jackson, H.R., Loudon, K.E., 2004. The limit of volcanic rifting: a structural model across the volcanic to non-volcanic transition off Nova Scotia (abstract): EOS. *Trans. Am. Geophys. Union* 85 Fall Meeting Supplement, T31D-04.
- Eagles, G., 2007. New angles on South Atlantic opening. *Geophys. J. Int.* 168, 353–361.
- Eagles, G., König, M., 2008. A model of plate kinematics in Gondwana breakup. *Geophys. J. Int.* 173, 703–717.
- Engen, O., Eldholm, O., Bungum, H., 2003. The arctic plate boundary. *J. Geophys. Res.* 108, 2075–2092.
- Eyles, N., Eyles, C.H., 1993. Glacial geologic confirmation of an intraplate boundary in the Parana basin of Brazil. *Geology* 21, 459–462.
- Franke, D., Neben, S., Ladage, S., Schreckenberger, B., Hinz, K., 2007. Margin segmentation and volcano-tectonic architecture along the volcanic margin off Argentina/Uruguay. *South Atlantic. Mar. Geol.* 244, 46–67.
- Franke, D., Ladage, S., Schnabel, M., Schreckenberger, B., Hinz, R.K., Paterlini, J., Siciliano, M., 2010. Birth of a volcanic margin off Argentina, South Atlantic. *Geochim. Geophys. Geosyst* 11, Q0AB04. <http://dx.doi.org/10.1029/2009GC002715>.
- Franke, D., 2013. Rifting, lithosphere breakup and volcanism: comparison of magma poor and volcanic rifted margins. *Mar. Pet. Geol.* 43, 63–87.
- Gaina, C., Torsvik, T.H., van Hinsbergen, D.J.J., Medvedev, S., Werner, S.C., Labails, C., 2013. The African Plate: a history of oceanic crust accretion and subduction since the Jurassic. *Tectonophysics* 604, 4–25.
- Gerya, T.V., 2013a. Initiation of transform faults at rifted continental margins: 3-d petrological-thermomechanical modeling and comparison to the Woodlark Basin. *Petrology* 21, 550–560.
- Gerya, T.V., 2013b. Three dimensional thermomechanical modeling of oceanic spreading initiation. *Phys. Earth Planet. Int.* 214, 35–52.
- Gladczenko, T.P., Hinz, K., Eldholm, O., Meyer, H., Neben, S., Skogseid, J., 1997. South Atlantic volcanic margins. *J. Geol. Soc.* 154, 465–470.
- Gladczenko, T.P., Skogseid, J., Eldholm, O., 1998. Namibia volcanic margin. *Mar. Geophys. Res.* 20, 313–341.
- Gradstein, F.M., Ogg, J.G., Smith, A.G., 2004. *A Geological Time Scale*, vol. 2004. Cambridge University Press, pp. 589.
- Gradstein, F.M., Ogg, J.G., Schmitz, M., Ogg, G., 2012. *The Geologic Time Scale*. Elsevier <http://dx.doi.org/10.1016/B978-0-444-59425-9.00005-6>.
- Granot, R., Dymant, J., 2015. The Cretaceous opening of the south Atlantic Ocean. *Earth Planet Sci. Lett.* 414, 156–163.
- Hall, S.A., Bird, D.E., 2007. Tristan da Cunha hotspot tracks and the seafloor spreading history of the South Atlantic (abstract): *Eos. Trans. Am. Geophys. Union* 88 Fall Meeting Supplement, V31F-04.
- Hall, S.A., Bird, D.E., Danque, H., Grant, J., McLean, D., Towle, P., 2014. New constraints on the age of the opening of the south Atlantic basin as revealed by recently acquired magnetic, gravity and seismic reflection data (abstract) *Eos. Trans. Am. Geophys. Union* 95 Fall Meeting Supplement, TC52C-03.
- Hayes, D.E., Manley, P.L., Malin, J.W., Houtz, R.E., 1991. Crustal structure: circum-Antarctic to 30°S. In: *Antarctic Research Series*, 54 In: Hayes, D.E. (Ed.), *Marine Geological and Geophysical Atlas of the Circum-Antarctic to 30°S*. American Geophysical Union, Washington D.C.
- Heine, C., Zoethout, J., Müller, R.D., 2013. Kinematics of the south Atlantic rift. *Solid Earth* 4, 215–253.
- Hey, R., 1977. A new class of “pseudofaults” and their bearing on plate tectonics: a rift propagating model. *Earth Planet Sci. Lett.* 37, 321–325.
- Hey, R., Duenebrier, F.K., Morgan, W.J., 1980. Propagating rifts on midocean ridges. *J. Geophys. Res.* 85, 3647–3658.
- Hinz, K., Neben, S., Schreckenberger, B., Roeser, H.A., Block, M., de Souza, K., Meyer, H., 1999. The Argentine continental margin north of 48°S: sedimentary successions, volcanic activity during breakup. *Mar. Pet. Geol.* 16, 1–25.
- Hirsch, K.K., Bauer, K., Scheck-Wenderoth, M., 2009. Deep structure of the western South African passive margin – results of a combined approach of seismic, gravity and isostatic investigations. *Tectonophysics* 470, 57–70.
- Johnston, S.T., 2000. The Cape Fold Belt and Syntaxis and the rotated Falkland Islands: dextral transpressional tectonics along the southwest margin of Gondwana. *J. Afr. Earth Sci.* 31, 51–63.
- Jokat, W., Boebel, T., König, M., Meyer, U., 2003. Timing and geometry of early Gondwana breakup. *J. Geophys. Res.* 108 EPM 4-1to 4-15.
- Jungslager, E.H.A., 1999. Petroleum habitats of the Atlantic margin of South Africa. In: Cameron, N.R., Bate, R.H., Clure, V.S. (Eds.), *The Oil and Gas Habitats of the South Atlantic*. vol. 153. Geological Society, London, pp. 153–168 Special Publications.
- Keen, C.E., Potter, D.P., 1995. The transition from a volcanic to non-volcanic rifted margin off eastern Canada. *Tectonics* 14, 3591–4371.
- Kington, J.D., Goodliffe, A.M., 2008. Plate motions and continental extension at the rifting to spreading transition in Woodlark Basin, Papua New Guinea: can oceanic plate kinematics be extended into continental rifts? *Tectonophysics* 458, 82–95.
- König, M., Jokat, W., 2006. The mesozoic breakup of the Weddell Sea. *J. Geophys. Res.* 111, BN12102. <http://dx.doi.org/10.1029/2005JB004035>.
- König, M., Jokat, W., 2010. Advanced insights into magmatism and volcanism of the Mozambique Ridge and Mozambique Basin in the view of new potential field data. *Geophys. J. Int.* 180, 158–180.
- Koopmann, H., Schreckenberger, B., Franke, D., Becker, K., Schnabel, M., 2014a. The late rifting phase and continental break-up of the southern South Atlantic: the mode and timing of volcanic rifting and formation of earliest oceanic crust. In: Wright, T.J., Ayele, A., Ferguson, D.J., Kidane, T., Vye-Brown, C. (Eds.), *Magmatic Rifting and Active Volcanism*. *Geol. Soc. London Special Publication* 420pp. 315–340.
- Koopmann, H., Franke, D., Schreckenberger, B., Schulz, H., Hartwig, A., Stollhofen, H., di Primo, R., 2014b. Segmentation and volcano-tectonic characteristics along the SW African continental margin, South Atlantic, as derived from multichannel seismic and potential field data. *Mar. Pet. Geol.* 50, 22–39.
- Kounov, A., Viola, G., de Wit, M.J., Andreoli, M., 2008. A Mid Cretaceous paleo-Karoo River valley across the Knersvlakte plain (northwest coast of South Africa): evidence from apatite fission-track analysis. *S. Afr. J. Geol.* 111, 409–420.
- LaBrecque, J.L., Hayes, D.E., 1979. Seafloor spreading history of the Agulhas basin. *Earth Planet Sci. Lett.* 45, 411–428.
- Larson, R.L., Hilde, T.W.C., 1975. A revised time scale of magnetic reversals for the early Cretaceous and late Jurassic. *J. Geophys. Res.* 80, 2586–2594.
- Larson, R.L., Ladd, J.W., 1973. Evidence for the opening of the south Atlantic in the early Cretaceous. *Nature* 246, 209–212.
- Lawver, L.A., Gahagan, L.M., Dalziel, I.W.D., 1998. A tight fit-early Mesozoic Gondwana, a plate reconstruction perspective. *Mem. Natl. Inst. Polar Res.* 53, 214–229 Special Issue.
- Leinweber, V.T., Jokat, W., 2012. The Jurassic history of the Africa-Antarctica corridor – new constraints from magnetic data on the conjugate continental margins. *Tectonophysics* 530–531, 87–101.
- Liao, J., Gerya, T., 2015. From continental rifting to seafloor spreading: insight from 3D thermo-mechanical modeling. *Gondwana Res.* 28, 1329–1343.
- Malinverno, A., Hildebrandt, J., Tominaga, M., Channell, J.E.T., 2012. M-sequence geomagnetic polarity time scale (MHTC12) that steadies global spreading rates and incorporates astrochronology constraints. *J. Geophys. Res.* 117, B06104.
- Martin, A.K., 1984. Propagating rifts: crustal extension during continental rifting. *Tectonics* 3, 611–617.
- Martin, A.K., Goodlad, S.W., Hartnady, C.J.H., du Plessis, A., 1982. Cretaceous palaeo-positions of the Falkland Plateau relative to southern Africa using Mesozoic seafloor spreading anomalies. *Geophys. J. Royal Astr. Soc.* 71, 567–579.
- Max, M.D., Ghidella, M., Kovacs, L., Paterlini, M., Valladares, J.A., 1999. Geology of the

- Argentine continental shelf and margin from aeromagnetic survey. *Mar. Pet. Geol.* 16, 41–64.
- McDonald, D., Gomez-Perez, I., Franzese, J., Spalletti, L., Lawver, L., Gahagan, L., Dalziel, I., Thomas, C., Trewin, N., Hole, M., Paton, D., 2003. Mesozoic break-up of SW Gondwana: implications for regional hydrocarbon potential of the southern South Atlantic. *Mar. Pet. Geol.* 20, 287–308.
- Moulin, M., Aslanian, D., Unternehr, P., 2010. A new starting point for the south and Equatorial Atlantic Ocean. *Earth Sci. Rev.* 98, 1–37.
- Müller, R.E., Roest, W.R., Royer, J.-Y., Gahagan, L.M., Sclater, J.G., 1997. Digital isochrons of the world's ocean floor. *J. Geophys. Res.* 102 (B2), 3211–3214.
- Nankivell, A.P., 1997. Tectonic Evolution of the Southern Ocean between Antarctica, South America and Africa over the Past 84 Ma. Doctor of Philosophy. University of Oxford, pp. 303.
- Nguyen, L.C., Hall, S.A., Bird, D.E., Ball, P.J., 2016. Reconstruction of the east Africa and Antarctica continental margins. *J. Geophys. Res.* 121 (B6), 4156–4179. <http://dx.doi.org/10.1002/2015JB012776>.
- Nürnberg, D., Müller, R.D., 1991. The tectonic evolution of the south Atlantic from late Jurassic to present. *Tectonophysics* 191, 27–53.
- Ogg, J.G., Ogg, G., Gradstein, F.M., 2016. A Concise Geologic Time Scale: 2016. Elsevier, Amsterdam B.V., The Netherlands, pp. 234.
- Paton, D.A., Mortimer, E.J., Hodgson, N., Van der Spuy, D., 2017a. The missing piece of the South Atlantic jigsaw: when continental breakup ignores crustal heterogeneity. In: Sabato Ceraldi, T., Hodgkinson, R.A., Backe, G. (Eds.), 2017. *Petroleum Geoscience of the West African Margin*, vol. 438. Geological Society, London, pp. 195–210 Special Publication.
- Paton, D.A., Pindell, J., McDermott, K., Bellingham, P., Horn, B., 2017b. Evolution of seaward-dipping reflectors at the onset of oceanic crust formation at volcanic passive margins: insights from the South Atlantic. *Geology* 45, 439–442.
- Pavlis, N.K., Holmes, S.A., Kenyon, S.C., Factor, J.K., 2012. The development and evaluation of the Earth gravitational model 2008 (EGM2008). *J. Geophys. Res.* 117, B04406.
- Perez-Diaz, L., Eagles, G., 2014. Constraining South Atlantic growth with seafloor spreading data. *Tectonics* 33. <http://dx.doi.org/10.1002/2014TC003644>.
- Pindell, J., Dewey, J.F., 1982. Permo-triassic reconstruction of Western pangea and the evolution of the Gulf of Mexico/caribbean region. *Tectonics* 1, 179–211.
- Quirk, D.G., Hertle, M., Jeppesen, J.W., Raven, M., Mohriak, W.U., et al., 2013. Rifting, subsidence and continental break-up above a mantle plume in the central South Atlantic. In: Mohriak, W.U., Danforth, A., Post, P.J., Brown, D.E., Tari, G.C. (Eds.), *Conjugate Divergent Margins*, vol. 369. Geological Society, London, pp. 185–214 Special Publications.
- Rabinowitz, P.D., 1976. Geophysical study of the continental margin of southern Africa. *Bull. Geol. Soc. Am.* 87, 1643–1653.
- Rabinowitz, P.D., LaBrecque, J., 1979. The mesozoic South Atlantic Ocean and evolution of its continental margins. *J. Geophys. Res.* 84 (B11), 5973–6002.
- Rey, S.S., Planke, S., Symonds, P.A., Faleide, J.I., 2008. Seismic volcanostratigraphy of the Gascoyne margin, Western Australia. *J. Vol. Geotherm. Res.* 172, 112–131.
- Sandwell, D.T., Müller, R.D., Smith, W.H.F., Garcia, E., Francis, R., 2014. New global marine gravity model from CryoSat-2 and Jason-1 reveals buried tectonic structure. *Science* 346, 65–67. <http://dx.doi.org/10.1126/science.1258213>.
- Sandwell, D.T., Smith, W.H.F., 1997. Marine gravity anomaly from Geosat and ERS 1 satellite altimetry. *J. Geophys. Res.* 102, 10039–10054.
- Schreckenberger, B., Hinz, K., Roeser, H.A., 1997. Magnetic modeling of seaward dipping reflector sequences: examples from the Atlantic volcanic margins. In: *ILP Volcanic Margins Workshop*, November 1997, Potsdam, Germany.
- Schreckenberger, B., Hinz, K., Franke, D., Neben, S., Roeser, H.A., 2002. Marine Magnetic Anomalies and the Symmetry of the Conjugated Rifted Margins of the South Atlantic. *AGU Fall Meet (Suppl.) T52C-1217* 1283.
- Talwani, M., Abreu, V., 2000. Inferences regarding initiation of oceanic crust formation from the U.S. East Coast margin and conjugate South Atlantic margins. In: Mohriak, W., Talwani, M. (Eds.), *Atlantic Rifts and Continental Margins*. Geophysical Monograph, vol. 115. American Geophysical Union, pp. 211–233.
- Taylor, B., Goodliffe, A.M., Martinez, F., 1999. How continents break up: insights from Papua New Guinea. *J. Geophys. Res.* 104, 7497–7512.
- Taylor, B., Goodliffe, A., Martinez, F., 2009. Initiation of transform faults at rifted continental margins. *Compt. Rendus Geosci.* 341, 428–438.
- Taylor, P.T., Zietz, I., Dennis, L.S., 1968. Geologic implications of aeromagnetic data for the eastern continental margin of the United States. *Geophysics* 33, 755–780.
- Tinker, J., de Wit, M., Brown, R., 2008. Mesozoic exhumation of the southern Cape, South Africa, quantified using apatite fission track thermochronology. *Tectonophysics* 455, 77–93.
- Tominaga, M., Sager, W., 2010. Revised Pacific M-anomaly geomagnetic polarity time-scale. *Geophys. J. Int.* 182, 203–232.
- Towle, P.J., McLean, D.J., Hall, S.A., Bird, D., Grant, J.V., Danque, H.A., 2015. New constraints on the early evolution of the south Atlantic basin as revealed by recently acquired magnetic, gravity and seismic reflection data: implications for hydrocarbon exploration along the SW African margin. In: *Extended Abstracts of the Petroleum Exploration Society of Great Britain (PESGB), Petroleum Exploration Society of Great Britain–Houston Geological Society (PESGB-HGS) Conference on African E&P: Always Something New Coming Out of Africa*, 3–4 September, Publ. PESGB, London, pp. 19–20.
- Torsvik, T.H., Rouse, S., Labails, C., Smethurst, M.A., 2009. A new scheme for the opening of the South Atlantic Ocean and the dissection of an Aptian salt basin. *Geophys. J. Int.* 177, 1315–1333.
- Tsikalas, F., Eldholm, O., Faleide, J.I., 2002. Early Eocene seafloor spreading and continent-ocean boundary between Jan Mayen and Senja fracture zones in the Norwegian-Greenland Sea. *Mar. Geophys. Res.* 23, 247–270.
- Unternehr, P., Curie, C., Olivet, J.L., Goslin, J., Beuzart, P., 1988. South Atlantic fits and intraplate boundaries in Africa and south America. *Tectonophysics* 155, 169–179.
- Van der Spuy, D., 2003. Aptian source rocks in some South African Cretaceous basins. In: Arthur, T.J., MacGregor, D.S., Cameron, N.R. (Eds.), *Petroleum Geology of Africa: New Themes and Developing Technologies*, vol. 207. Geological Society, London, pp. 185–202 Special Publications.
- Vink, G.E., 1982. Continental rifting and the implications for plate tectonic reconstructions. *J. Geophys. Res.* 87, 10677–10688.